

Cool topoclimates promote cold-adapted plant diversity in temperate mountain forests.



Jeremy Borderieux^{1,2}, Emiel De Lombaerde^{3,4}, Karen De Pauw⁴, Pieter Sanczuk⁴, Pieter Vangansbeke⁴, Thomas Vanneste⁴, Pieter De Frenne⁴, Jean-Claude Gégout¹, Josep M. Serra-Diaz^{1,5}.

1. Université de Lorraine, AgroParisTech, INRAE, UMR Silva, 54000 Nancy, France.
2. Department of Forest and Conservation Sciences, Faculty of Forestry, University of British Columbia, Vancouver, British Columbia, Canada
3. Research Institute for Nature and Forest (INBO), Brussels, Belgium
4. Forest & Nature Lab, Department of Environment, Ghent University, Geraardsbergsesteenweg 267, 9090 Gontrode, Belgium.
5. Botanical Institute of Barcelona (IBB, CSIC - CMCNB), 08038 Barcelona, Spain.

Orcid ID:

Jeremy Borderieux : 0000-0003-3993-1067

Emiel De Lombaerde : 0000-0002-0050-2735

Karen De Pauw : 0000-0001-8369-2679

Pieter Sanczuk : 0000-0003-1107-4905

Pieter Vangansbeke : 0000-0002-6356-2858

Thomas Vanneste : 0000-0001-5296-917X

Pieter De Frenne : 0000-0002-8613-0943

Jean-Claude Gégout : 0000-0002-5760-9920

Josép M. Serra-Diaz: 0000-0003-1988-1154

Corresponding author: Jeremy Borderieux: jeremy.borderieux@ubc.ca

Abstract

Climate strongly influences the composition and diversity of forest plant communities. Recent studies have highlighted the role of tree canopies in shaping understory thermal conditions at small spatial scales (i.e. microclimate), especially in lowland forests. In mountain forests, however, the influence of topography in environmental conditions (i.e., topoclimate) is ought to also influence plants' perceived temperature. Understanding how topography and canopies interactively affect understory temperature is key to identifying stable refugia that could shelter cold-adapted forest specialist plants under climate change.

Here we report on growing season understory temperatures using 48 loggers in contrasting topographic features and canopy of a mid-range mountain valley spanning from 475 m a.s.l. to 1203 m a.s.l. in the Vosges Mountains (NE France). We disentangle the relative importance and the effects of topography vs. canopy in determining local temperatures. We then evaluate how topography and canopy-induced variation in temperature drive plant community composition and richness in 306 floristic surveys across the studied mountain valley.

Our results show that topography outweighed canopy cover in explaining growing season understory temperatures. Regardless of canopy, the daily mean temperature of the growing season in south-facing ridges was 1.5 °C (CI: 0.62 - 2.38°C) warmer than shaded valley bottoms, while dense canopies cooled temperatures by 0.5 °C (CI: 0.02 - 0.98 °C) compared to less dense canopies. Topoclimate explained community composition as much as elevation and was the only significant predictor of species richness. Cold topoclimate harbored 30% more species than the average species richness across our plots. This increase in species richness was explained by an increase of cold-adapted species, both forest specialist and generalist species.

Our findings highlight a stronger role of topography compared to canopy cover on community composition in mountain forests via topoclimatic cooling of north-facing slopes and valley bottoms. The importance of topographic features to explain temperature cooling and diversity underpins their role as present and likely future microrefugia.

Keywords

Community ecology, forest, topoclimate, microclimate, topography, climatic refugia, diversity, understory vegetation.

1. Introduction

The study of topography influences on vegetation has fascinated ecologists for more than 150 years (Johnston *et al.*, 1848), and has further gained in relevance in the context of the 21st century climate warming (Ashcroft, 2010; Dobrowski, 2011; IPCC, 2021; Lenoir *et al.*, 2017). Species distribution and climatic conditions are often modeled at a coarse resolution (typically 1 km or coarser), and thereby fail to capture local variation of climate at finer grains (Franklin *et al.*, 2013): for instance, the topoclimate shaped by terrain (i.e. slope and aspect mainly) and the forest-induced microclimate (Bramer *et al.*, 2018; De Frenne *et al.*, 2021; Kemppinen *et al.*, 2023). Enhanced predictive power obtained by using smaller grain climatic data confirms that species physiological limits are better captured by topography and forest microclimate (Haesen *et al.*, 2023). Given that these factors can attenuate warm macroclimate temperatures, their study is key to identify areas where local conditions are continually buffered in a warmer future (Ashcroft, 2010; De Frenne *et al.*, 2021; Haesen *et al.*, 2023; Hannah *et al.*, 2014). Such areas, refugia, are of utmost importance as they can host source populations of cold-adapted species endangered by climate change. Protection offered by these refugia can be disrupted in when it is induced by tree canopies whereas topography-induced buffering is more stable (Ashcroft, 2010; Hylander *et al.*, 2022). As these buffer components coexist in temperate mountainous forests, determining which buffering process is at play will allow to better predict and map sources of biodiversity persistence.

Variation in aspect can create contrasting local temperatures as slopes oriented to the equator receive more solar radiation, and west-facing slopes receive radiation during the warmest period of the day. As a result, southwest-facing slopes in northern hemisphere mountains display warmer mean temperatures, longer growing seasons and shorter snow cover durations (Ashcroft *et al.*, 2008; Davis *et al.*, 2019; Rita *et al.*, 2021; Rolland, 2003). The physical properties of air also interact with topographic features such as hydrological basins (McLaughlin *et al.*, 2017), valley bottoms and sinks. This phenomenon creates local areas of cold and dense air pooling that decouple, i.e. remove any correlation, between local conditions from the regional climate (Gudiksen *et al.*, 1992; Pastore *et al.*, 2022), thus creating topographic refugia (Dobrowski, 2011). These temperature variations are observed on a moderate scale, from fifty to hundreds of meters, and will be called hereafter topoclimate (Lenoir *et al.*, 2013). To focus on moderate scale and magnitude variation in temperature, we exclude from our definition of topoclimate the lapse rate induced from elevation, as this process has a much stronger effect on temperature, comparable to macroclimatic variation (Lenoir *et al.*, 2013; Rolland, 2003).

The topoclimate interacts with what we define as forest-induced microclimate (with smaller scale variation, from a meter to 25 m) to jointly determine the understory temperature experienced by forest organisms (De Frenne *et al.*, 2021). Canopy shading and evapotranspiration lead to an overall decrease of temperature throughout the year,

exacerbated in summer by a buffering of high temperatures compared to open-air (De Frenne *et al.*, 2021; Zellweger, Coomes, *et al.*, 2019). These buffering effects are apparent and well documented in temperate lowland forests, but their relative importance in contrast to elevation and topography is less known, and current evidence has not reached consensus (Macek *et al.*, 2019; Vandewiele *et al.*, 2023). In temperate mountain forests, we expect that topography (elevation excluded) displays more variability than canopy cover, placing it as the main driver of understory temperature and thus community composition.

Community composition was proven to respond to canopy cover in lowland forests. This is evidenced by the decrease of the average thermal optimum of the present species (a proxy of species' affinity to climate) in forests where tree canopy is densifying (De Frenne *et al.*, 2013; Dietz *et al.*, 2020; Richard *et al.*, 2021) and where colder understory temperatures are predicted (Zellweger *et al.*, 2020). This sheltering of cold-adapted species by a dense canopy needs to be compared with the sheltering provided by topography in mountain forests, as topographical refugia are likely to offer longer-term buffering of temperature, whereas canopy cover is prone to sudden perturbation (dieback, windfall, etc.) (Ashcroft, 2010; Finocchiaro *et al.*, 2023). Topographic refugia also harbor cold-adapted flora and host populations of species outside their expected climatic range (Ellis & Eaton, 2021; Finocchiaro *et al.*, 2023; Haesen *et al.*, 2023; Macek *et al.*, 2019). Less known is how variation in temperature owing to topography and canopy cover can influence local diversity. No change in diversity will indicate a reshuffling of community with microclimate, however we expect an increase in diversity as a moderate cooling can relieve cold-adapted species stress and competition without inducing dieback in species not adapted to cold conditions. In temperate mountain forests, it is possible that the sheltering provided by topography resembles the effect of canopy (e.g. lower maximum temperature, higher humidity). To test this hypothesis, we will also study the species' characteristics, expecting an increase of forest specialists that could demonstrate that topoclimate can mimic understory conditions of dense forests.

Here, we assessed the effects and relative importance of elevation, topography and canopy cover on *in situ* measured understory temperatures and plant community composition and richness. This partitioning will shed light on whether communities are more responsive to canopy or topographic variability, processes that have very different spatial and temporal patterns. This will allow conservation planning to efficiently target conservation areas. After accounting for the elevation gradient, we specifically asked: (1) Does topography (aspect and topographic position) outweigh canopy in explaining understory temperature? (2) does topography and canopy-induced variation in temperature determine community richness and mean species thermal optimum? (3) Are plant habitat preference and climatic affinity related to understory temperature?

2. Materials and Methods

2.1. Study Area

Our study region (221 km²) is delineated by the basin of the Thur River, located in one of the southmost valleys of the Vosges Mountain range in France (Figure 1). The Vosges are characterized by a continental climate with harsh winters and short and stormy summers. Its mean annual temperature ranges from 6 °C to 10 °C and precipitation ranges from 800 to 2,000 mm year⁻¹ (period 1970-2000, Météo France weather stations IGN, 2013). The Thur River basin is on the warm and dry end gradient of the Vosges Mountains (IGN, 2013). Forests cover 76% of the Vosges, which transitions from mixed oak stands and monospecific *Picea abies* stands to mixtures of *Picea abies*, *Abies alba* and *Fagus sylvatica* as elevation increases (IGN, 2013). The soil of our study region is mostly shallow loam and sand with coarse elements. The most acidic soils are found at higher altitude because of the dominance of needles in the humus and the lower temperature at mountaintops (IGN, 2013; Piqué *et al.*, 1994; Thomas *et al.*, 1999). The topography is highly variable, with an elevation ranging from 327 to 1424 m a.s.l. (but forest occurrence stops past 1250 m a.s.l.) with high topographic heterogeneity (Figure 1, Figure S1).

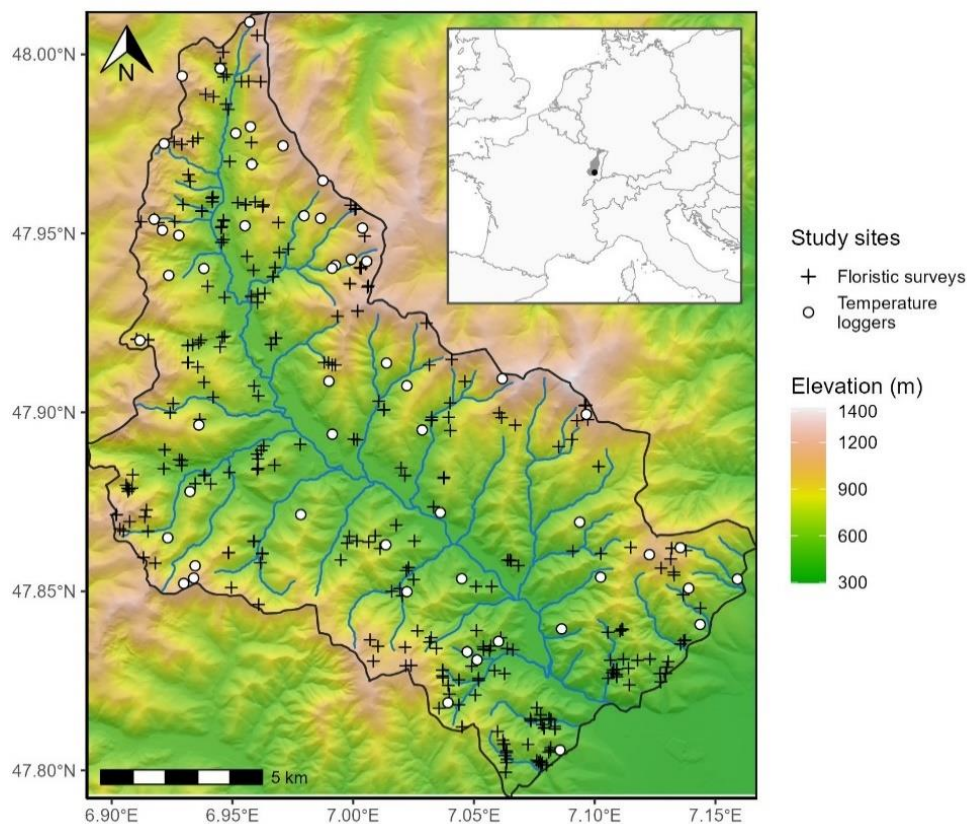


Figure 1: Study area (black outline) with the location of the temperature loggers (white circles) and the floristic surveys (black crosses). The colored scale represents elevation above sea level, in meters, obtained from a 25-m spatial resolution digital elevation model

(IGN, 2017). Hillshade effects have been added to visualize the terrain. The blue line represents the Thur River and its tributaries. The inset shows the Vosges Mountain range (grey) and the location of the studied valley (black point) in western Europe.

2.2. Temperature Predictors

We used 25-meter resolution digital elevation model (IGN, 2017) to extract elevation (m a.s.l.), slope and aspect and to calculate topographical indices. Elevation was kept as is, as the lapse rate predictor, but does not fall under our definition of topography as we considered it a macroclimatic feature given how much control it has over temperature. This is evidenced by spatial autocorrelation (semivariance) of elevation saturating at a distance ten times greater than small scale topographic features (Figure S2). Accordingly, our definition of topoclimatic effect will be focused on smaller scale topographic features described hereafter. We specifically wanted to investigate the difference in radiation received between slopes of differences aspects, a well know driver of topoclimate temperatures, which its effect is less clear under canopy (Macek *et al.*, 2019). We did so by computing the Heat Load Index (HLI). HLI ranges from 0 to 1 (least to most incoming solar radiation) contingent on latitude, slope orientation and steepness. It is a measure of how daily mean temperature is warmed by topographic features most exposed to sunlight, and during the warmest period of the day (south and west slope in the northern hemisphere).

To investigate how cold air pooling, dictated by the topography of river basins, influences temperature, we computed a topographic position index (TPI). Cold air pooling ought to be a prominent explanatory factor of community persistence (Finocchiaro *et al.*, 2023; Pastore *et al.*, 2022). To do so, we normalized the Euclidian distance between the nearest ridge and nearest thalweg ($TPI = D_{thalweg} / (D_{thalweg} + D_{ridge})$). TPI is the relative position of the cell in the shortest trajectory between a ridge and a drainage basin end, ranging from 0 (valley bottom) to 1 (ridge, Piedallu *et al.*, 2023).

We obtained the ‘tree cover density’ from the 2018 product of the Copernicus monitoring service as proxy for local canopy closure (Copernicus, 2018; Sannier *et al.*, 2023). This product consists of a 10-meter resolution percentage of canopy presence within the pixel (ranging from 0 to 100%) and was successfully used before to model microclimate buffering by canopy (Haesen *et al.*, 2021). To validate the assumption that this is a proxy of local canopy closure, and thus microclimatic variation induced by canopy, we correlated it with our field measurements of canopy closure (see below, 2.3 Temperature sampling). We rescaled this product to match the 25-m resolution of our other maps using bilinear interpolation (Hijmans, 2020). We rasterized (25-meter resolution) a 20-meter precision polygon map of French forest (IGN, 2019) to create a mask of the forested area of our study region to limit our analysis and temperature projection to forests, as we only investigate understory flora and temperatures in this study.

Our in our study region, within forested areas, our elevation ranges from 327 to 1362 m a.s.l., HLI ranges from 0.16 to 1, TPI from 0 to 1, slope from 0.1 to 50° and canopy closure

from 0 (temporary deforested) to 1 (Figure S1). Variation in canopy closure was hover low, as 90% of the cells display a canopy closure higher than 72% (Figure S1), this indicates that the remote sensed product we use may not reflect finer scale gaps in canopy.

2.3. Temperature Sampling

We created a stratified sampling scheme to capture forest understory microclimate variability (Lembrechts *et al.*, 2021; Schweiger *et al.*, 2016). We created 8 elevation strata (spanning 20 m a.s.l. intervals) separated by 102 m. Those strata thus range from [468 - 488] to [1184 - 1204] m a.s.l. They are meant to control for the lapse rate (steady decrease in air temperature as pressure decreases with elevation, Lembrechts *et al.*, 2021), it is the main driver of temperature in the study area but we wanted to separate lapse rate from other topographic features effect.

Inside each of these strata, we defined 8 types of plots: 4 plots of below and above the median canopy closure of our study area (90% canopy closure) with a south or a north-facing slope ($HLI > 0.70$ and $HLI < 0.60$, respectively, value chosen to avoid flat terrains of $HLI: 0.66$). These 4 plots had moderate topographic position indices (between 0.2 and 0.8) and slope ($10^\circ < \text{slope} < 25^\circ$), to avoid confounding their effects with the canopy closure and heat load effects. Additionally, we defined 2 plots with contrasting topographic position indices (lower than 0.2 and higher than 0.8) under high canopy closure and moderate slope. Lastly, we defined 2 plots with contrasting slopes: one on flat ($\text{slope} < 10^\circ$) and one steep ($\text{slope} > 25^\circ$) under high canopy closure and moderate topographic position (summary of the sampling scheme:

Table S1). These theoretical strata and plots were designed to systematically cover elevation, HLI, TPI and canopy closure variability, yielding similar results as the PCA-based approach proposed in Lembrechts *et al.*, 2021 as shown in Figure S3.

Of the initial 64 theoretical plots spanning the 8 strata, only 59 of the defined situations occurred, mostly because we lacked low topographic position indices (valley bottom) in high elevation classes. We randomly selected one cell for each plot and stratum located in public forests. We repeated this random drawing 10,000 times and kept the set of plots that maximized the mean minimum geographical distance between plots to reduce spatial autocorrelation.

We established the 59 temperature loggers in May 2021 and recorded their location with a GNSS receiver (Trimble TDC600, accuracy= ± 2 m undercover). We placed every logger in public forests to avoid legal constraints (public forest makes up 80% of the forested area in our study region), with no constraints regarding accessibility. We measured canopy closure (0-100%) by a visual observation in a 25-meter radius around the logger. We also estimated canopy closure (0-100%) with a planar picture of the canopy by means of a smartphone (Samsung A40, focal length: 25mm, sensor size: 1/2.8") placed on top of the logger and the

sky segmentation ‘*Glama*’ application (Tichý, 2016). Plots tagged as low canopy cover were placed accordingly by selecting sites with less than 50% canopy closure as computed by ‘*Glama*’. The visual estimation of canopy closure (25-meter radius) was significantly correlated with the remote sensed tree density (R^2 of the linear relationship = 30.0%, Figure S4), but a weak and non-significant correlation was found with the picture analyzed by ‘*Glama*’ (Figure S4).

We recorded air and soil temperatures with TMS-4 loggers (resolution= 0.0625 °C, accuracy= ± 0.5 °C) protected with a radiation shield (Wild *et al.*, 2019). The loggers recorded temperature every 15 minutes until August 2022. We used air temperature 15 cm above the soil surface because it is likely the most representative temperature experienced by understory plants. We cleaned the time series with the ‘*myClim*’ R package (Man *et al.*, 2023). More specifically, we removed any duplicates, checked for missing values, and resolved inconsistent time step to the closest 15 minutes default of our loggers. We calibrated the loggers beforehand for a range of -20 °C to +40 °C by placing them in a freezer and drying oven along with a T-type thermocouple (accuracy= ± 0.2 °C). From the recorded period, we focused on the growing season (GS hereafter), from 01/04/2023 to 15/08/2023, as it is the most critical period for plant growth. Out of the 59 loggers, 11 were either malfunctioning, stolen, destroyed by animals or displayed erroneous values and were discarded.

We checked the capacity of our final sample to cover the variability of our study region following the PCA-based approach of Lembrechts *et al.*, (2021). Our final sampling was able to cover the variability of the valley, except for extreme values of low canopy cover and the unusual valley bottoms of high elevations. The loss of loggers was evenly distributed over plot types, except for the low canopy cover that suffered the most losses (Figure S3).

2.4. Floristic and Species Characteristic Dataset

To test how flora responded to understory temperature, we compiled floristic surveys performed (during the growing season) by students and professors covering soil and climatic transect of the region between 2009 and 2022 (average year= 2015.6). All plots were surveyed for all vascular plant species in the herb layer (smaller than 1 m) and their percentage ground cover was visually estimated. We had 306 floristics surveys in total across the study region. Floristic surveys were performed in 20 x 20 m squares (400 m²) with the GPS position (recorded with built-in tablet GPS; accuracy= ± 10 m) as the center. We used this position to extract elevation, heat load index, topographic position index and canopy cover for every survey. We harmonized taxonomy to the TaxRef V13 standard (Gargominy, 2022). We focused on herbaceous species in the analysis to focus on community dynamics that may reflect shorter-term climate while not being directly targeted by forest management interventions.

One of the objectives of our study is to assess whether local variation of temperature due to topography and canopy benefits cold-adapted species, as they are projected to be the most threatened by climate warming (Thuiller *et al.*, 2005). For this purpose, we used the species' thermal optimum value from ClimPlant V.1.2 (Vangansbeke *et al.*, 2021). These thermal optima are computed from the mean annual temperature (°C) within the range of species obtained from Europe-extent distribution atlases and represent the median temperature of the realized niche. Out of the 348 unique recorded species, 309 were assigned a thermal optimum value, covering 90.0% of the occurrences of the whole floristic dataset. We averaged the thermal optimum of every species (without weighting for abundance) of a given survey to obtain the Community Thermal Index (hereafter CTI), which quantifies the thermal preference of the whole community (Borderieux *et al.*, 2023; Vangansbeke *et al.*, 2021). We did not weigh the calculation by species abundance, from a conservation standpoint rarer species may be the most interesting in CTI calculation but may be underrepresented when weighted by abundance. We calculated species richness of a plot as the number of recorded species whether they had an associated thermal optimum in the database or not. By doing so, we wanted to include rare species that were not included in ClimPlant so that our specific richness is representative of the species pool of our study region. The soil of our study region can greatly vary in acidity, we also assigned a pH optimum value obtained from a bioindication database to each species (Gégout *et al.*, 2005), and averaged (not weighted by abundance) it to obtain to control for soil conditions via a bioindicated pH per plot.

We used the EuForPlant regional list of forest plant species (Heinken *et al.*, 2022) to assess species habitat affinity. We assigned to each species one of the following affinities: (1.1) species of closed forest (1.2) species which occur in forest edges and openings (2.1) Species which primarily occur in forests but also found in cultural landscapes and forest remnants (2.2) species of open habitats that occurs in forest exclusively through opening and early succession. We excluded species of open vegetation (classified "O") because of their low number of occurrences (n= 42). In total, 274 species were assigned to an affinity class, covering 85.7% of the occurrences.

2.5. Understory Temperature Modeling

We aggregated the 15-minute frequency time series of the recorded temperature of the growing season 2022 (a warmer than average year, see 3.1) to daily mean and maximum temperature. This aggregation process first removed values outside of the 5th to 95th centile interval of daily values to avoid biasing results due to logger malfunction or a brief burst of sunshine on a logger (thus maximum temperature is the 95th centile). We then averaged the mean or maximum daily temperature to obtain one unique value per logger, the mean daily and maximum daily temperature of the growing season. Having a unique value facilitates the modeling process by removing the need to account for the lack of statistical dependence of temperature time series, and one summary value of the GS is enough as we aim to uncover spatial variation of community composition instead of temporal variation.

We wanted to disentangle the relative contribution of lapse rate, topography and canopy to understory temperature, and wanted to map estimates of understory over the study area. To this end, we used a linear model to predict mean and maximum daily temperature of the growing season with elevation, heat load index, topographic position index and remote sensed canopy density as explanatory variables. We preferred remote-sensed canopy cover over the *in-situ* measurements which allowed us to map the temperature models over the entire study area, and thus infer the understory temperature of floristic surveys (mostly without canopy closure records). The warming due to radiation can be tempered when there is canopy to intercept light, canopy buffering is most apparent during the warmest hour of the day (Davis *et al.*, 2019; De Frenne *et al.*, 2021). To account for this, we tested an interaction between heat load index and canopy closure and retained the interaction in the final model if found significant. We checked the assumption of linearity between temperature and its predictors by visually assessing the raw data (Figure S5) and the residuals (Zuur & Ieno, 2016). The Variance Inflation Factor never exceeded 1.2 in our understory temperature models, indicating no sign of correlation among predictors.

For each understory temperature model, we did an analytical partitioning of variance to assess which process influenced understory temperature most (Barbosa *et al.*, 2013). The contribution of the predictors was grouped into three groups: elevation, “topoclimate” (TPI and HLI) and “microclimate” (canopy closure). For simplicity and because shared effects had little contribution, we added to each group contribution half of their shared effect to summarize the contribution of the three groups in three numbers.

We additionally fitted two linear models with the field measured canopy closure (25 m radius observation and planar photography) instead of the remotely sensed measurement to test different methods of canopy closure estimations (Table S2, Table S3).

We used the mean understory temperature model ($R^2 = 92.2\%$) to map the contribution of elevation (i.e., lapse rate), of topoclimate (heat load index and topographic position) and of forest-induced microclimate (canopy closure) to the mean understory temperature separately. We mapped the lapse rate by using only the intercept and the elevation parameter. We mapped the topography effect on temperature compared to a reference situation (heat load index of a flat terrain = 0.66 and topographic position index equal to 0.5, prediction of + 1.34°C) and using the two topographic indices. We mapped the contribution of canopy cover by multiplying its parameter to the tree density product, this projection is however extrapolated for the 20% of pixels with a canopy closure lower than 79%. This extrapolation was necessary to cover the whole study region and to predict temperature to floristic surveys within those areas. To assess the spatial autocorrelation of the resulting maps (Figure S2), we computed their variogram (scaled semivariance), with a lag of 25 m and a cutoff of 2000 m (Naimi *et al.*, 2014).

2.6. Floristic Composition Analyses

We used a linear model to predict CTI. Species richness being a positive discrete number, we used a negative binomial generalized linear model as overdispersion prevented the use of a Poisson model. The predictors of both models were the contribution to mean understory temperature of elevation, topoclimate and microclimate (the unit of every predictor is thus °C). The soil of our study region can display very different nutrition status and acidity, which can impact both the richness and composition of a community (Degen et al., 2005; Koerner et al., 1997; Zellweger et al., 2015). In addition, soil pH is also negatively correlated with elevation (Pearson coefficient: 0.40, Piqué et al., 1994; Thomas et al., 1999). To account for this, bioindicated pH was also a predictor in the models. We tested that no collinearity between soil acidity and elevation arose when including both by computing a Variance Inflation Factor (VIF, Fox & Weisberg, 2019). For both models, elevation displayed the higher VIF (1.27, well below the threshold of 5, that indicates collinearity, James et al., 2023).

We assessed the validity of our models (including temperature models) by testing the assumption of normality and homoscedasticity of the residuals model following (Zuur & Ieno, 2016). All assumptions were met (Figure S6), all the P-values of the Kolmogorov-Smirnov test, dispersion test and outlier test of the normalized Dharma residuals were not significant (Hartig, 2024). We tested the significant difference from 0 of the estimated parameters with a Wald test.

As the 306 surveys uniformly covered the topography effect on temperature (Figure S7), we could split them into three classes of 102 surveys corresponding to a “cold”, “moderate” and “warm” topoclimate effect (a linear prediction of contribution to temperature by TPI and HLI as there was no interaction with canopy cover). The thresholds separating the three classes were determined so that classes have equal number of plots. This discretization allows to directly compare the total occurrence of species, as in Figure 4, thanks to a fixed sampling intensity between classes. It also allows to compute more comprehensive effects of topoclimate over CTI and species richness (e.g. “cold” plots exhibit on average 5 more species than “warm” plots) than with linear estimates. We tested the difference in species richness and CTI between these classes with Wilcoxon rank-sum tests (Rey & Neuhäuser, 2011).

2.7. Software

We handled spatial data with the ‘*raster*’ and ‘*sf*’ package (Hijmans, 2020; Pebesma, 2018), all the later analyses were carried on with R.4.2.2 (R Core Team, 2019). We computed HLI (McCune & Keon, 2002) using the ‘*spatialEco*’ R package (Evans & Murphy, 2021). We used the ‘*MASS*’ package to fit the negative binomial generalized model (Venables & Ripley, 2002). We computed the VIF using the ‘*car*’ package (Fox & Weisberg, 2019). Microclimate temperatures were cleaned using the ‘*myClim*’ R package (Man et al., 2023). We used ‘*ggplot2*’ and ‘*ggspatial*’ packages for data visualization (Dunnington & Thorne, 2020;

Wickham, 2011). We performed variance partitioning with the ‘*modEVA*’ package (Barbosa *et al.*, 2013).

3. Results

3.1. Environmental Determinant of the Understory Temperature

The growing season (GS) temperature of 2022 was above average (mean GS temperature of the period 2005-2020=11.6 °C, mean 2022 GS temperature=13.2 °C, Markestein weather station (1,184 m a.s.l), (Météo France, 2024)). As a result, the mean daily temperature of the understory (15 cm above the soil surface) was 14.6 °C and spanned between 11.9 °C to 17.5 °C for the higher (1203 m a.s.l) and lower (475 m a.s.l) elevation sensors, respectively. The mean daily maximum temperature of the GS was 19.3 °C and reached a maximum of 24.7 °C for the lowest elevation plots.

The lapse rate explained 87.4% of the variation in mean temperature, the topographic factors (heat load and topographic position index) 3.95%, and canopy cover accounted for 0.82%. The R^2 of the linear model was 92.2%. Elevation was the primary driver of mean temperature variation, with a lapse rate estimated at -0.68 °C by 100m (Table 1). The model revealed that HLI - contingent on aspect and slope - was the second driver of mean temperature, which can vary up to 1 °C between low and high radiation slopes. Topographic position also had a significant effect on temperature: the mean temperature was 0.56 °C lower in the bottom of a valley compared to ridges. Lastly, canopy closure (remotely sensed) cooled understory temperatures. An increase of 20% of total canopy cover resulted in a decrease of 0.57 °C. No significant interaction between topography features metric and canopy closure was found in the mean and maximum understory temperature model.

The same predictors except for topographic position were significant in the mean daily maximum temperature model, but the model explained overall less variation (R^2 of 81.2 %). The heat load index had a higher contribution (21.5%) in the maximum temperature compared to the mean temperature model, daily maxima varied for 3.3 °C between low and high heat load indices (Table S4). Canopy closure has a stronger effect (contribution to R^2 of 3.2%) on maximum temperature than on mean temperature.

Same models where remotely-sensed canopy closure was replaced with field-measured canopy closure showed overall similar trends, but with difference in estimates significance. Canopy cover visually estimated in a 25-meter radius was not significant in predicting mean temperature (Table S2). Immediate canopy cover (smartphone photography) above the logger explained significantly mean temperature with an interaction with heat load index, low immediate canopy cover in high radiation slopes displayed warmer mean temperature (Table S3).

Table 1: Estimated parameters, their standard error and p-values of the predictors included in models of the daily mean growing season temperature. The range of the predictors in

*the calibration dataset and their standardized effect size on the temperature (standard deviation * estimate) are displayed. The percentage of explained variation per type of predictor is included. P-values were obtained with a Wald test on parameters. Heat load and topographic position have no units (n.u., refer to the methods for their calculation).*

Predictor	Type of predictor	Estimate	Standard error	Range	Effect size (°C)	Explained variation (%)	P-value
Intercept (°C)		21,1	1,11				<10 ⁻⁴
Elevation (m a.s.l.)	Elevation	-0.00684	0.000311	475 : 1203	-1.50	87.4	<10 ⁻⁴
Heat load index (n.u)	Topoclimate	1.53	0.333	0.34 : 0.95	0.30	3.95	<10 ⁻⁴
Topographic position (n.u)		0.656	0.276	0.15 : 1	0.16		0.0220
Canopy closure (%)	Microclimate	-0.0272	0.0115	79.0: 100	-0.16	0.817	0.0229

The spatial variation of elevation, topography and canopy closure reveals a complex and fine-grained contribution of this factors to the forest understory climate (Figure 2). We mapped the individual contributions of elevation (Figure 2.a), topoclimate (heat load index and topographic position summed; Figure 2.b) and canopy cover (i.e., microclimate; Figure 2.c) in the study area. We observed strong effects on understory temperatures caused by steep spatial difference of elevation, topography and fine-grained canopy cover (Figure 2.d). Lapse rate autocorrelation peaked at 6000 m, while topography in was autocorrelated in a moderate scale 750 m, canopy-induced variation in temperature autocorrelated in the smallest scale and peaked at 450 m (Figure S2).

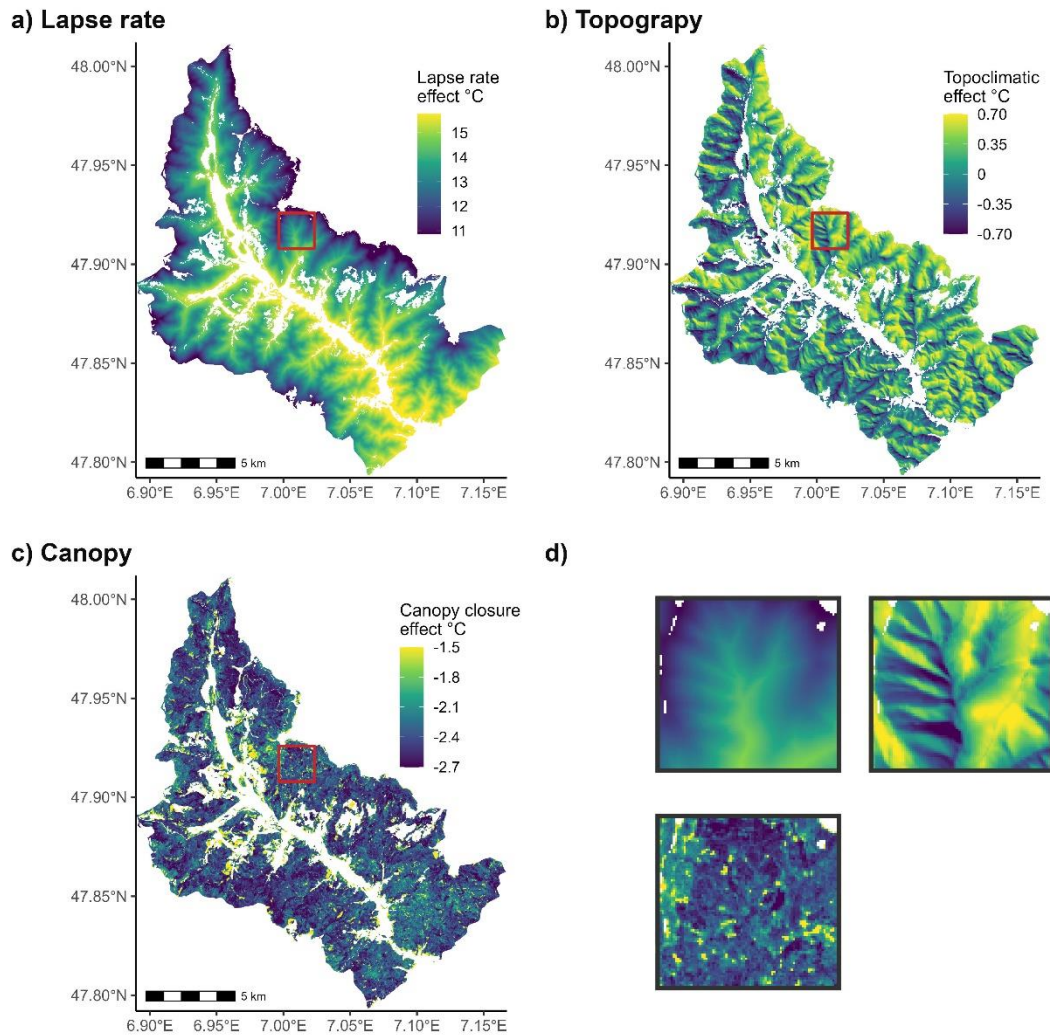


Figure 2: a) Elevation induced change in mean growing season understory temperature of the growing season (lapse rate of $-0.68^{\circ}\text{C}\cdot 100\text{ m}^{-1}$), assuming a canopy closure of 90% and no effect from topography. b) mean understory temperature effect induced by topography (heat load and topographic position, i.e. topography) assuming an average canopy cover (90%), compared to a moderate situation (flat terrain midslope). c) mean understory temperature cooling induced by canopy closure assuming no effect from topography. For visualization purposes only we restrained the minimal cooling to -1.5°C , however some pixels displayed lower values up to 0°C due to low canopy closure. d) 2 km per 2 km zoomed inset of the red square of the other panels, their color gradient corresponds to the color scale presented in the other panels a-c, respectively. Blank pixels represent land covers other than forests or forests outside of the study region. Linear model R^2 : 92.2%.

3.2. Microclimatic Determinants of the Floristic Composition

Floristic surveys harbored on average 19 herbaceous species (s.d. 10.7), and a mean community thermal index (CTI) of 7.8°C (s.d. 0.55). Bioindicated soil pH was the main predictor of CTI and species richness (Table 2). More acidic soils had less diverse and cold-adapted communities. The overall linear CTI model explained a moderate amount of variability (R^2 : 35.6%).

After soil pH, elevation-induced (lapse rate) and topoclimate were the main predictor of CTI, of comparable importance (effect size of 0.14 and 0.12 respectively). Topographic effect was also a significant predictor of species richness, of major importance (an increase of 1.5 species per plot per decrease, of one standard deviation of topographic effect on temperature, i.e., cooling, Table 2). The lapse rate was not significant in explaining species richness (Table 2). The forest-induced microclimate was not a significant predictor in any of the models (Table 2). We focused the subsequent community analysis around topoclimatic effects, as canopy cooling did not significantly explain the species richness nor CTI.

Mean and maximum temperature were highly correlated (Pearson coefficient: 0.86), as a result, a similar effect on flora is found when using predicted effect on max temperature instead of mean temperature, with a small decrease in fit quality (-1.4% in R^2 for CTI model, -6 in log-likelihood for the species richness model, Table S5).

*Table 2: Estimated parameters, their standard error and p-values of the predictors of the community thermal index (CTI) linear model, and the species richness negative binomial generalized linear model. The range of the predictors and their standardized effect size on the community predicted variable (standard deviation * estimate) are displayed. The P-value is obtained by a Wald test on the parameter.*

Model	Predictor	Estimate	Standard error	Range	Effect size	P-value
Species richness	Intercept (°C)	0.212	0.403			0.598
	Lapse rate (°C)	0.0218	0.0187	12.6 : 18.5	0.46	0.243
	Topography effect (°C)	-0.38	0.0795	-1.55 : -0.13	-1.50	<10 ⁻⁴
	Canopy cooling (°C)	0.0439	0.121	-2.72 : -1.31	0.13	0.716
	Bioindicated pH	0.406	0.0315	3 : 7.15	5.2	<10 ⁻⁴
Community Thermal Index (°C)	Intercept (°C)	5.18	0.406			<10 ⁻⁴
	Lapse rate (°C)	0.0885	0.0188	12.6 : 18.5	0.14	<10 ⁻⁴
	Topography effect (°C)	0.364	0.0804	-1.55 : -0.13	0.12	<10 ⁻⁴
	Canopy cooling (°C)	-0.0236	0.123	-2.72 : -1.31	-0.049	0.848
	Bioindicated pH	0.272	0.0308	3 : 7.15	0.25	<10 ⁻⁴

We divided the 306 floristic surveys into cold, moderate and warm topoclimatic classes each comprised of 102 surveys based on topography-induced change in temperature. The cold topoclimatic class displayed 23 species on average, while the two other classes displayed 18.5 species on average (Figure 3.a). This difference of approximately 5 species was significantly different (Figure 3.a). The mean CTI of the cold topoclimatic class was 7.7 °C, which is significantly lower by 0.19 °C than the CTI of the two other classes (Figure 3.b). No such differences were found when using microclimatic (canopy) cooling was used to create the classes (Figure S8). This discretization of the dataset displayed results as those observed using the continuous predictors of the linear model (Table 2, Figure S7).

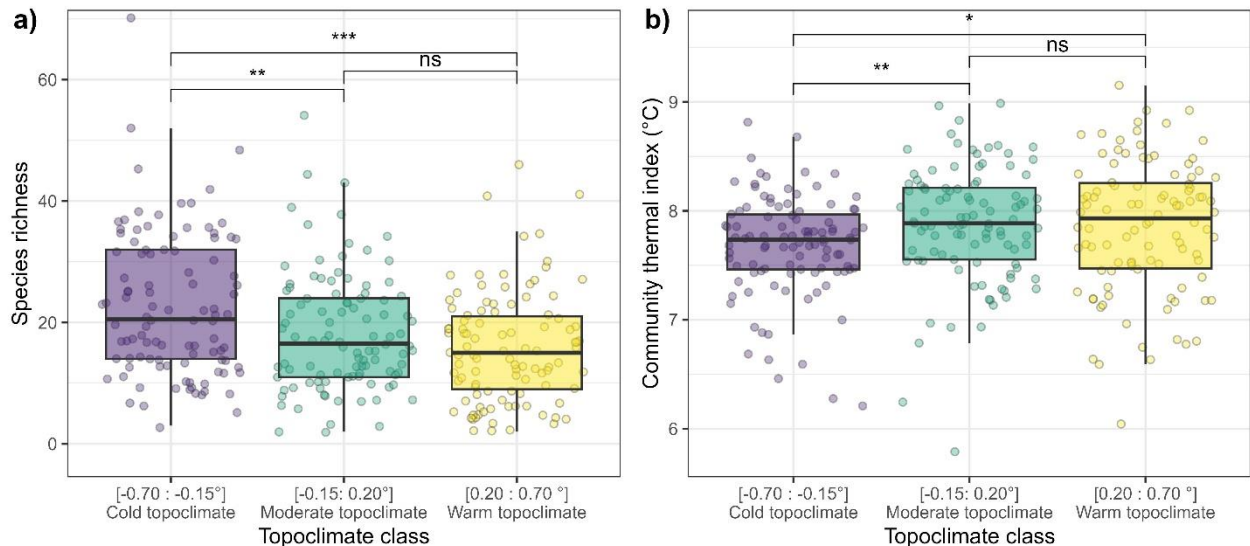


Figure 3: Species richness (a) and community thermal index (b) of 306 floristic surveys evenly spread into three topoclimate classes of even number of plots (n=102 species by class). The p-value significance of a Wilcoxon test between two classes is displayed as follows: (ns): $p > 0.05$ (*): $p < 0.05$ (**): $p < 0.01$ (***): $P < 0.001$.

The decreases in CTI and the increase in species richness in the cold topoclimatic class were explained by a surplus of relatively cold-adapted species (i.e. with a species thermal optimum of 9 °C or less) (Figure 4.a). A two-sided Kolmogorov-Smirnov test confirmed that the distribution of species thermal optimum in the cold topoclimate class is significantly different from the other two (P-value against warm= $< 10^{-6}$, P-value against moderate = 0.00282). No difference in distribution was found between the warm and moderate class (P-value = 0.18). The plots (n=102 vegetation surveys) in cold topoclimates displayed in total more than 50 to 100 more occurrences of relatively cold-adapted species per thermal optimum classes (1°C) than the other two categories (Figure 4.a). The intermediate topoclimatic class (n=102) also had a higher number of cold-adapted species compared to the warm topoclimatic class (n=102, Figure 4.a). The cold topoclimatic class displayed 300 more forest-specialist species occurrences (Heinken *et al.*, 2022) than the other warmer topoclimatic classes, whereas the occurrences of generalist species increased by 200 in total (Figure 4.b). We recorded a total of 246, 242 and 223 species (i.e., species pool) in the cold, intermediate and warm topoclimatic classes, respectively. A total of 58, 41, and 33 species were unique to the cold, intermediate and warm topoclimatic classes, respectively. This means that there are nestedness of species between communities, as shown in Figure S9.

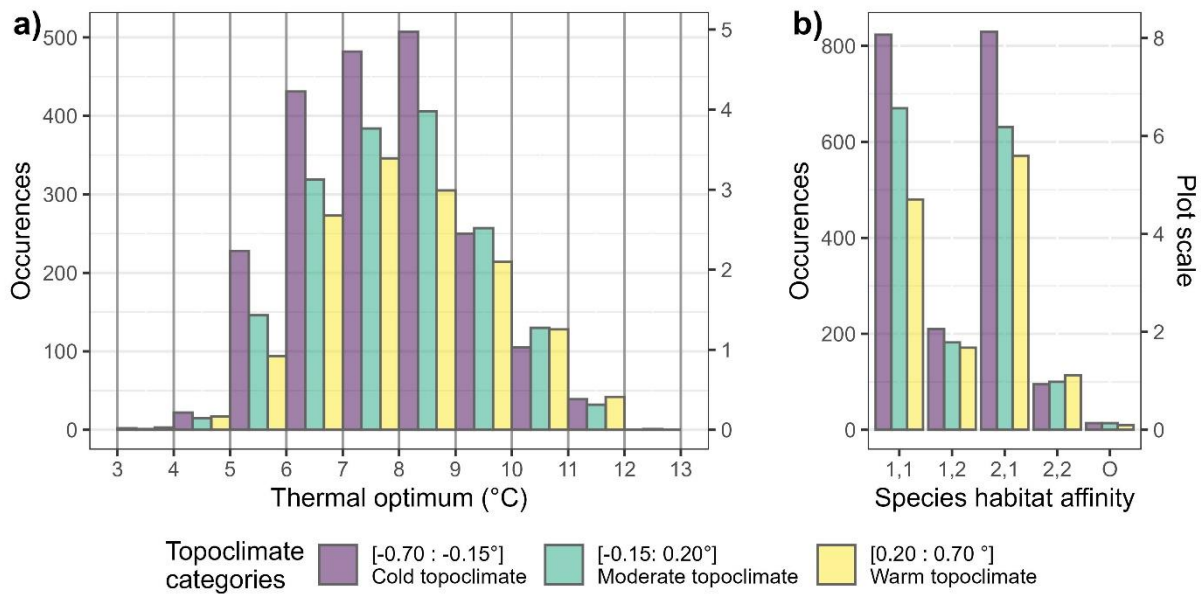


Figure 4: Occurrences of species in the three topoclimatic classes as a function of a) their thermal optimum ($^{\circ}\text{C}$) and b) their habitat affinity defined by the EuForPlant list as follows: 1,1: closed forest mainly 1,2: forest edges and opening 2,1: forest and open vegetation 2,2: mainly in open vegetation (Heinken et al., 2022) The plot-scale occurrence of species is also shown (e.g., 400 occurrences corresponds to approximately 4 species per plots).

4. Discussion

We found that both canopy cover and topographic factors strongly influenced (without interacting) understory temperature during the growing season. We disentangled the elevation gradient from the topoclimatic and canopy-induced factors by estimating the lapse rate separately, which was expectably the main driver of understory temperature (Figure 2). After controlling for the lapse and pH, the temperature cooling by topographic factors (Heat load and topographic position) was the only significant driver of community composition and richness. Our understory temperature model allowed us to separately predict the lapse rate, topoclimatic effect and canopy cover cooling with mean temperature as a unit. This allows inferring direct links between temperature variation and communities, a necessary step to advance correlative studies.

4.1. Understory temperature determinants

The positive correlation found between temperature and heat load can be attributed to the higher radiation an equator-facing slope receives, which increases both the mean and daily maximum temperature of the growing season in closed forests. This contrasts with a previous study which only found an effect of heat load on maximum temperature (Macek *et al.*, 2019). We measured temperature at 15 cm above the surface, which may explain the higher sensitivity of mean GS temperature to aspect compared to Macek *et al.*, (2019), who measured temperature at 2 m above the surface. Alongside heat load, we found that topographic position influenced mean temperature so that ridges were warmer, and valley bottoms were cooler (given equal elevation) but had no effect on maximum temperature.

We attribute this decrease in temperature to cold air pooling that occurs during nighttime, thus influencing mean daily temperature but with a minimal effect during the hottest hour of the day, when air temperature is homogeneously warm (Smith *et al.*, 2010; Vosper & Brown, 2008). The cooling effect of understory temperature by canopy cover was most apparent for maximum temperature but was also significant for mean temperature, although with a small effect size of -0.16 °C. These observations concur with studies with comparable sampling (Davis *et al.*, 2019; Macek *et al.*, 2019).

We found that topoclimatic factors outweighed canopy closure in explaining understory temperature in our study area. This finding adds to the current divergent results from Macek *et al.*, (2019) who found no effect of canopy and Vandewiele *et al.*, (2023) who found a predominance of canopy control on temperature in mountain forests. These apparent contrasting results illustrate the complexity of factors in mountain forest microclimates, potentially depending on site-specific variations in topography and canopy cover, alongside with synoptic conditions leading to difference in transmittance. Our sampling design and subsequent loss of loggers hampered our ability to capture the canopy closure gradient effect on temperature. In our effort of representativeness, our “low canopy” plots displayed a remotely sensed canopy closure of 75%, as there was a dramatic decrease of pixels with values lower than that (Figure S9). However, Zellweger *et al.*, (2019) showed that temperature canopy cooling is more apparent at low canopy cover levels, and saturates past 80% canopy cover. Our limited number of loggers below that threshold could also be the reason why we did not observe a strong effect of canopy on temperature. We argue that our results are interpretable as a comparison of topographic and canopy effects within already forested stands, but not as a comparison of open and closed forests. In previous iterations of the temperature models, we tried to account for the ration of broadleaved and evergreen canopy trees (Díaz-Calafat *et al.*, 2023) but found no significant effect. This could be due to the study period of the growing season, representing leaf-on conditions and thus reducing the difference in canopy buffering induced by lack of leaves in leaf-off conditions.

Part of the challenge to determine canopy cover controls in mountain forests stems from the myriads of methods that are used to estimate canopy cover, ranging from hemispheric photographs, terrestrial lidar derived metrics to remotely sensed canopy cover estimations (Ma *et al.*, 2017; Zellweger, De Frenne, *et al.*, 2019). We used Copernicus tree density 2018 satellite images to calibrate the microclimatic model and predict its buffering effect on communities. Remote sensed tree closure density does not account for the vertical profile of trees, which have profound influence on sunlight interception and consequently on understory temperatures (Gril *et al.*, 2023; Zellweger, Coomes, *et al.*, 2019). Remotely sensed canopy cover was significantly but poorly correlated with our field measures (visual estimation and photography). This poor correlation could increase uncertainty in subsequent prediction of canopy-induced change in temperature, making more difficult to study community composition and richness. Consistent hemispheric photography of loggers and

vegetation plots, or remote sensed lidar offers appealing alternatives to better capture canopy closure variation independent of the topography context.

We fitted additional understory temperature models with in-situ measurements of canopy cover to conservatively reject canopy cover as prominent driver of microclimate and consequently community composition. These models showed no correlation between understory temperatures and canopy closure except from the interaction between immediate canopy closure (photography) and Heat Load Index (Table S2,

Table S3). Previous studies have shown that a localized lack of canopy has stronger warming effect when being located in equator-facing slopes (Davis et al., 2019; Rita et al., 2021). This explains why our most local measure of canopy closure only shows a significant interaction. This demonstrates the need to simultaneously study multiple microclimatic drivers and their interactions in mountain ranges (Davis et al., 2019; Greiser et al., 2020).

4.2. Understory temperature effect on communities

We found that temperature variation owing to topography was equally important in shaping a community's affinity to climate compared to that of the elevational gradient (Table 2, after soil pH has been controlled for). This is likely a consequence of environmental selection pressure on community assembly. Lower temperature at higher altitudes or in topographically shaded slopes can exert a selection pressure on species not adapted to cold whereas lower elevation and high radiation slopes select species not sensitive to late freezing and adapted to warmer temperature (Figure 3, Rita et al., 2021; Wei et al., 2024). Our prediction of both elevation and topography control on mean temperature are quantified the same unit, Celsius degrees °C, but topography-induced temperature effect on community composition is fourfold compared to that of elevation (Table 2). This implies that temperature alone cannot drive the difference in community composition, and other biophysical factors correlated with topography-induced temperature should be at play. Maximum temperature could be a better predictor of the crossing of physiological thresholds dictating species selection (Macek et al., 2019; Pérez-Navarro et al., 2021). However, this hypothesis could not be tested with our dataset as mean and maximum understory temperature were highly correlated. Soil moisture and vapor pressure deficit can also explain the important contribution of topography to communities (Davis et al., 2019).

Our topographic position metric relies on hydrography, demonstrating that cold air pooling could occur alongside wetter soils and synergistically favor cold-adapted species not tolerant to drought (Bénichou & Le Breton, 1987; Finocchiaro et al., 2023; Raduła et al., 2018). Conversely, ridges and south facing slopes exacerbate the effect of warmer temperature by desiccation, via stronger winds and evaporation, respectively (Davis et al., 2019; Piedallu et al., 2023; Rita et al., 2021). These underlying factors altogether can also explain the differences we found in contribution to community composition. They underscore the potential in using several microclimate variables (e.g., mean temperature, vapor pressure deficit) to predict community patterns and species distribution, explicitly

considering other microscale biophysical factors in a multivariate fashion (Pérez-Navarro *et al.*, 2021). The improvement of mechanistic modeling of microclimate (Maclean, 2020) could also improve predictions of present and future community composition.

The cold-adapted communities we observed in cold topoclimates are the result of an increase in relatively cold-adapted species occurrences rather than of a decrease in relatively warm-adapted species (Figure 3). This hints that the constraints on community assembly, in our study region, are a result of temperature becoming too warm for cold-adapted species, rather than otherwise. This increase in occurrences explains the higher specific richness in cold topoclimates (Figure 3). Further to an understory cooling, colder topoclimates could also increase moisture, thus alleviating competition for water during summer and allowing more species to co-occur (Raduła *et al.*, 2018; Sanceruk *et al.*, 2022). Canopy cover has been identified as the driver of the diversity of many taxa in lowland forests due to its buffering of microclimate and light interception (Tinya *et al.*, 2021; Zellweger *et al.*, 2015). Its lower contribution to microclimate variation in mountain forests and the limitation in its measurement mentioned earlier may explain why we do not detect this pattern.

Aside from the technical limitations in estimating canopy control on temperature we discussed above, other factors may be at play in explaining the lack of flora response to canopy-induced microclimate. It was outside of the scope of our analysis but explicitly unveiling seasonal microclimatic differences from leaf out timing can help uncover fine community differences such as presence of species vulnerable to cold winter, late freezing and spring ephemeral species. We also showed that after the lapse rate and topoclimate, canopy-induced microclimate is the most variable in space (i.e., spatially autocorrelated in smaller scale, Figure S2). A recent study has shown that plant's thermal preference computed with macroclimate are not responsive to microscale variation in temperature, but rather reflect macroclimatic provenance differences (Gril *et al.*, 2024). Surprisingly, topography, a moderate spatial scale contributor of temperature, had an important effect on these macroscales estimate of plant thermal preference. This demonstrates that topoclimate, being more stable in space and time, can promote cold-adapted species comparably to a macroclimate gradient.

4.3. Implications

How local cooler and wetter conditions are decoupled from the climate warming trend is of utmost importance as they allow for the persistence of cold-adapted species (Greiser *et al.*, 2020; Lenoir *et al.*, 2017), or provide opportunities to facilitate colonization and facilitates range shifts (Serra-Diaz *et al.*, 2015). The thermal heterogeneity topoclimate produced in mountain ranges (Figure 2) should also be considered as a driver of landscape-scale diversity (Stein *et al.*, 2014) and a potential source of community adaptation because species of diverging climatic adaptation coexist in a relatively small area (Hylander *et al.*, 2022; Lenoir *et al.*, 2013, 2013). More specifically, our results support the “identifying and

protecting microrefugia” section highlighted by Hylander *et al.*, (2022), as north-facing slopes and topographic depressions are easily identifiable from maps, and their cooling capacities and cold-adapted communities can be confirmed by visits in the field.

The predominance of topoclimate as a driving force of community composition and richness allows for potential stable refugia to occur. Indeed, buffering of community by canopy alone is prone to disturbances (e.g., increased mortality of trees triggered by climate change) and the magnitude of the buffering effect on community is still under scrutiny (Bertrand *et al.*, 2020). Still, a continuity of tree cover in cold topoclimate is recommended, as it ultimately creates the understory microclimate that benefits from such topographic effects. This could be achieved through selective logging and continuous cover silviculture and the reduction of edge effects thanks to buffer zones around the microrefugia. Topography displaying higher control over communities shows that targeting cold topoclimates is an efficient conservation strategy than increasing canopy density in already closed forests. Conservation targeting cold topoclimates is more robust because of the increase in redundancy and biodiversity those locations provide (Figure S9). Additionally, maintaining a connected forest will foster the benefits of the thermal heterogeneity created by topography (Hylander *et al.*, 2022). Indeed, warm topoclimates ought to serve as source populations of species adapted to the current climate, and cold topoclimates have the potential to maintain cold-adapted populations (given sufficient buffering and areas wide enough to sustain a population), resulting in a landscape with heterogenous communities.

In summary, we show that elevation, topography, and to a lesser extent, canopy closure determines growing season understory temperature in the Vosges mountains in France. Besides elevation, the contribution of topoclimate was the main predictor of community composition and diversity. Understory plant communities of cold topoclimates (north facing slopes and valley bottoms) harbored a higher number of generalist and forest specialist cold-adapted species. Our results place topography as a prominent driver of forest temperature and a key factor to consider for protecting forest cold-adapted species in the context of accelerated global warming.

5. Acknowledgment

This preprint has been reviewed and recommended through PCI Ecology, the review history and recommendation can be found here: <https://doi.org/10.24072/pci.ecology.100749>.

The authors are grateful to the Grand Ventron naturel reserve and its director Laurent Domergue for the permission to access the core of the protected forest. The authors acknowledge the National Office for Forests (ONF) for permission to place loggers in public forests. The authors thank the AgroParisTech students and professors involved in the collection of floristic data. The authors thank the funding from a PHC Tournesol mobility grant N° 47550SB. JB Acknowledge the funding from a joint funding from Region Grand Est and AgroParisTech (19_GE8_01020p05035), and was also supported by a ERC synergy grant

RESILIENCE (101071417). JMSD was funded by the ANR-JCJC (Agence Nationale de la Recherche, jeunes chercheuses et jeunes chercheurs) SEEDFOR (ANR-21-CE32-0003). JMSD acknowledges the support from NASA for UConn's Ecological Modelling Institute (#80NSSC 22K0883) and the program RYC2022-035668-I, funded by MCIU/AEI/10.13039/501100011033 and FSE+.

The authors of this preprint declare that they have no financial conflict of interest with the content of this article.

6. Data availability

The spatial, microclimatic, and floristic data used for this analysis can be found in the repository: https://github.com/Jeremy-borderieux/Article_microclim_vosges.git, and in the archive: <https://zenodo.org/records/12626861> along with the R script that can be used to reproduce the analyses and the figures.

7. References

- Ashcroft, M. B. (2010). Identifying refugia from climate change: Identifying refugia from climate change. *Journal of Biogeography*. <https://doi.org/10.1111/j.1365-2699.2010.02300.x>
- Ashcroft, M., Chisholm, L., & French, K. (2008). The effect of exposure on landscape scale soil surface temperatures and species distribution models. *Faculty of Science - Papers (Archive)*, 211-225. <https://doi.org/10.1007/s10980-007-9181-8>
- Barbosa, A. M., Real, R., Munoz, A. R., & Brown, J. A. (2013). New measures for assessing model equilibrium and prediction mismatch in species distribution models. *Diversity and Distributions*, 19(10), 1333-1338. <https://doi.org/10.1111/ddi.12100>
- Bénichou, P., & Le Breton, O. (1987). Prise en compte de la topographie pour la cartographie de champs pluviométriques statistiques: La méthode Aurelhy. *Colloques de l'INRA*, 39(51-69).
- Bertrand, R., Aubret, F., Grenouillet, G., Ribéron, A., & Blanchet, S. (2020). Comment on "Forest microclimate dynamics drive plant responses to warming". *Science*, 370(6520). <https://doi.org/10.1126/science.abd3850>
- Borderieux, J., Gégout, J.-C., & Serra-Diaz, J. M. (2023). High landscape-scale forest cover favours cold-adapted plant communities in agriculture-forest mosaics. *Global Ecology and Biogeography*, 32(6), 893-903. <https://doi.org/10.1111/geb.13676>
- Bramer, I., Anderson, B. J., Bennie, J., Bladon, A. J., De Frenne, P., Hemming, D., Hill, R. A., Kearney, M. R., Körner, C., Korstjens, A. H., Lenoir, J., Maclean, I. M. D., Marsh, C. D., Morecroft, M. D., Ohlemüller, R., Slater, H. D., Suggitt, A. J., Zellweger, F., & Gillingham, P. K. (2018). Chapter Three—Advances in Monitoring and Modelling Climate at Ecologically Relevant Scales. In D. A. Bohan, A. J. Dumbrell, G. Woodward, & M. Jackson (Éds.), *Advances in Ecological Research* (Vol. 58, p. 101-161). Academic Press. <https://doi.org/10.1016/bs.aecr.2017.12.005>
- Copernicus. (2018). *High Resolution Layer Tree Cover Density* [Data set]. <https://land.copernicus.eu/en/products/high-resolution-layer-tree-cover-density>
- Davis, F. W., Synes, N. W., Fricker, G. A., McCullough, I. M., Serra-Diaz, J. M., Franklin, J., & Flint, A. L. (2019). LiDAR-derived topography and forest structure predict fine-scale variation in daily surface temperatures in oak savanna and conifer forest landscapes. *Agricultural and Forest Meteorology*, 269-270, 192-202. <https://doi.org/10.1016/j.agrformet.2019.02.015>

- De Frenne, P., Lenoir, J., Luoto, M., Scheffers, B. R., Zellweger, F., Aalto, J., Ashcroft, M. B., Christiansen, D. M., Decocq, G., De Pauw, K., Govaert, S., Greiser, C., Gril, E., Hampe, A., Jucker, T., Klinges, D. H., Koelemeijer, I. A., Lembrechts, J. J., Marrec, R., ... Hylander, K. (2021). Forest microclimates and climate change: Importance, drivers and future research agenda. *Global Change Biology*. <https://doi.org/10.1111/gcb.15569>
- De Frenne, P., Rodriguez-Sanchez, F., Coomes, D. A., Baeten, L., Verstraeten, G., Vellend, M., Bernhardt-Romermann, M., Brown, C. D., Brunet, J., Cornelis, J., Decocq, G. M., Dierschke, H., Eriksson, O., Gilliam, F. S., Hedl, R., Heinken, T., Hermy, M., Hommel, P., Jenkins, M. A., ... Verheyen, K. (2013). Microclimate moderates plant responses to macroclimate warming. *Proceedings of the National Academy of Sciences*, 110(46), 18561-18565. <https://doi.org/10.1073/pnas.1311190110>
- Degen, T., Devillez, F., & Jacquemart, A.-L. (2005). Gaps promote plant diversity in beech forests (Luzulo-Fagetum), North Vosges, France. *Annals of Forest Science*, 62(5), 429-440. <https://doi.org/10.1051/forest:2005039>
- Díaz-Calafat, J., Uria-Diez, J., Brunet, J., De Frenne, P., Vangansbeke, P., Felton, A., Öckinger, E., Cousins, S. A. O., Bauhus, J., Ponette, Q., & Hedwall, P.-O. (2023). From broadleaves to conifers: The effect of tree composition and density on understory microclimate across latitudes. *Agricultural and Forest Meteorology*, 341, 109684. <https://doi.org/10.1016/j.agrformet.2023.109684>
- Dietz, L., Collet, C., Dupouey, J.-L., Lacombe, E., Laurent, L., & Gégout, J.-C. (2020). Windstorm-induced canopy openings accelerate temperate forest adaptation to global warming. *Global Ecology and Biogeography*. <https://doi.org/10.1111/geb.13177>
- Dobrowski, S. Z. (2011). A climatic basis for microrefugia: The influence of terrain on climate. *Global Change Biology*, 17(2), 1022-1035. <https://doi.org/10.1111/j.1365-2486.2010.02263.x>
- Dunnington, D., & Thorne, B. (2020). ggspatial: Spatial Data Framework for ggplot2. *R package version 1, 1*.
- Ellis, C. J., & Eaton, S. (2021). Climate change refugia: Landscape, stand and tree-scale microclimates in epiphyte community composition. *The Lichenologist*, 53(1), 135-148. <https://doi.org/10.1017/S0024282920000523>
- Evans, J. S., & Murphy, M. A. (2021). *spatialEco*. <https://github.com/jeffreyevans/spatialEco>
- Finocchiaro, M., Médail, F., Saatkamp, A., Diadema, K., Pavon, D., & Meineri, E. (2023). Bridging the gap between microclimate and microrefugia: A bottom-up approach reveals strong climatic and biological offsets. *Global Change Biology*, 29(4), 1024-1036. <https://doi.org/10.1111/gcb.16526>
- Fox, J., & Weisberg, S. (2019). *An R Companion to Applied Regression* (Third). Sage. <https://www.john-fox.ca/Companion/>
- Franklin, J., Davis, F. W., Ikegami, M., Syphard, A. D., Flint, L. E., Flint, A. L., & Hannah, L. (2013). Modeling plant species distributions under future climates: How fine scale do climate projections need to be? *Global Change Biology*, 19(2), 473-483. <https://doi.org/10.1111/gcb.12051>
- Franklin, J., Serra-Diaz, J. M., Syphard, A. D., & Regan, H. M. (2016). Global change and terrestrial plant community dynamics. *Proceedings of the National Academy of Sciences*, 113(14), 3725-3734. <https://doi.org/10.1073/pnas.1519911113>
- Gargominy, O. (2022). *TAXREF v13.0, référentiel taxonomique pour la France*. [Data set]. UMS PatriNat (OFB-CNRS-MNH), Paris. <https://doi.org/10.15468/VQUEAM>
- Gégout, J.-C., Coudun, C., Bailly, G., & Jabiol, B. (2005). EcoPlant: A forest site database linking floristic data with soil and climate variables. *Journal of Vegetation Science*, 16(2), 257-260. <https://doi.org/10.1111/j.1654-1103.2005.tb02363.x>

- Greiser, C., Ehrlén, J., Meineri, E., & Hylander, K. (2020). Hiding from the climate : Characterizing microrefugia for boreal forest understory species. *Global Change Biology*, 26(2), 471-483. <https://doi.org/10.1111/gcb.14874>
- Gril, E., Laslier, M., Gallet-Moron, E., Durrieu, S., Spicher, F., Le Roux, V., Brasseur, B., Haesen, S., Van Meerbeek, K., Decocq, G., Marrec, R., & Lenoir, J. (2023). Using airborne LiDAR to map forest microclimate temperature buffering or amplification. *Remote Sensing of Environment*, 298, 113820. <https://doi.org/10.1016/j.rse.2023.113820>
- Gril, E., Spicher, F., Vanderpoorten, A., Vital, G., Brasseur, B., Gallet-Moron, E., Le Roux, V., Decocq, G., Lenoir, J., & Marrec, R. (2024). Ecological indicator values of understorey plants perform poorly to infer forest microclimate temperature. *Journal of Vegetation Science*, 35(2), e13241. <https://doi.org/10.1111/jvs.13241>
- Gudiksen, P. H., Leone, J. M., King, C. W., Ruffieux, D., & Neff, W. D. (1992). Measurements and Modeling of the Effects of Ambient Meteorology on Nocturnal Drainage Flows. *Journal of Applied Meteorology and Climatology*, 31(9), 1023-1032. [https://doi.org/10.1175/1520-0450\(1992\)031<1023:MAMOTE>2.0.CO;2](https://doi.org/10.1175/1520-0450(1992)031<1023:MAMOTE>2.0.CO;2)
- Haesen, S., Lembrechts, J. J., De Frenne, P., Lenoir, J., Aalto, J., Ashcroft, M. B., Kopecký, M., Luoto, M., Maclean, I., Nijs, I., Niittynen, P., van den Hoogen, J., Arriga, N., Bruna, J., Buchmann, N., Čiliak, M., Collalti, A., De Lombaerde, E., Descombes, P., ... Van Meerbeek, K. (2021). ForestTemp - Sub-canopy microclimate temperatures of European forests. *Global Change Biology*, 27(23), 6307-6319. <https://doi.org/10.1111/gcb.15892>
- Haesen, S., Lenoir, J., Gril, E., De Frenne, P., Lembrechts, J. J., Kopecký, M., Macek, M., Man, M., Wild, J., & Van Meerbeek, K. (2023). Microclimate reveals the true thermal niche of forest plant species. *Ecology Letters*, 26(12). <https://doi.org/10.1111/ele.14312>
- Hannah, L., Flint, L., Syphard, A. D., Moritz, M. A., Buckley, L. B., & McCullough, I. M. (2014). Fine-grain modeling of species' response to climate change : Holdouts, stepping-stones, and microrefugia. *Trends in Ecology & Evolution*, 29(7), 390-397. <https://doi.org/10.1016/j.tree.2014.04.006>
- Hartig, F. (2024). *DHARMA: Residual Diagnostics for Hierarchical (Multi-Level / Mixed) Regression Models*. <https://CRAN.R-project.org/package=DHARMA>
- Heinken, T., Diekmann, M., Liira, J., Orczewska, A., Schmidt, M., Brunet, J., Chytrý, M., Chabrierie, O., Decocq, G., De Frenne, P., Dřevojan, P., Dzwonko, Z., Ewald, J., Feilberg, J., Graae, B. J., Grytnes, J.-A., Hermy, M., Kriebitzsch, W.-U., Laiviņš, M., ... Vanneste, T. (2022). The European Forest Plant Species List (EuForPlant) : Concept and applications. *Journal of Vegetation Science*, 33(3), e13132. <https://doi.org/10.1111/jvs.13132>
- Hijmans, R. J. (2020). *raster : Geographic Data Analysis and Modeling*. <https://CRAN.R-project.org/package=raster>
- Hylander, K., Greiser, C., Christiansen, D. M., & Koelemeijer, I. A. (2022). Climate adaptation of biodiversity conservation in managed forest landscapes. *Conservation Biology*, 36(3), e13847. <https://doi.org/10.1111/cobi.13847>
- IGN. (2013). *Fiches descriptives des grandes régions écologiques (GRECO) et des sylvoécórégions (SER)*. <https://inventaire-forestier.ign.fr/spip.php?article773>
- IGN. (2017). *BD ALTI Le modèle numérique de terrain (MNT) maillé qui décrit le relief du territoire français à moyenne échelle [Data set]*. <https://geoservices.ign.fr/documentation/donnees/alti/bdalti>
- IGN. (2019). *BD Forêt version 2*. Institut National de l'Information Géographique et Forestière. <https://inventaire-forestier.ign.fr/spip.php?article646>
- IPCC. (2021). Summary for Policymakers. In V. Masson-Delmotte, P. Zhai, A. Pirani, S. L. Connors, C. Péan, S. Berger, N. Caud, Y. Chen, L. Goldfarb, M. I. Gomis, M. Huang, K. Leitzell, E. Lonnoy, J. B. R. Matthews, T. K. Maycock, T. Waterfield, O. Yelekçi, R. Yu, & B. Zhou (Éds.), *Climate Change 2021: The Physical Science Basis*.

- Contribution of Working Group I to the Sixth Assessment Report of the Intergovernmental Panel on Climate Change* (p. 3–32). Cambridge University Press. <https://doi.org/10.1017/9781009157896.001>
- James, G., Witten, D., Hastie, T., Tibshirani, R., & Taylor, J. (2023). *An Introduction to Statistical Learning: With Applications in Python*. Springer International Publishing. <https://doi.org/10.1007/978-3-031-38747-0>
- Johnston, A. K., Brewster, D., & Berghaus, H. K. W. (1848). *The physical atlas: A series of maps & notes illustrating the geographical distribution of natural phenomena* [Map]. William Blackwood & Sons.
- Kempinen, J., Lembrechts, J. J., Van Meerbeek, K., Carnicer, J., Chardon, N. I., Kardol, P., Lenoir, J., Liu, D., Maclean, I., Pergl, J., Saccone, P., Senior, R. A., Shen, T., Słowińska, S., Vandvik, V., von Oppen, J., Aalto, J., Ayalew, B., Bates, O., ... De Frenne, P. (2023). *Microclimate, an inseparable part of ecology and biogeography*. Zenodo. <https://doi.org/10.5281/zenodo.7973314>
- Koerner, W., Dupouey, J. L., Dambrine, E., & Benoit, M. (1997). Influence of Past Land Use on the Vegetation and Soils of Present Day Forest in the Vosges Mountains, France. *Journal of Ecology*, 85(3), 351-358. <https://doi.org/10.2307/2960507>
- Lembrechts, J. J., Lenoir, J., Scheffers, B., & De Frenne, P. (2021). Designing countrywide and regional microclimate networks. *Global Ecology and Biogeography*. <https://doi.org/10.1111/geb.13290>
- Lenoir, J., Graae, B. J., Aarrestad, P. A., Alsos, I. G., Armbruster, W. S., Austrheim, G., Bergendorff, C., Birks, H. J. B., Bråthen, K. A., Brunet, J., Bruun, H. H., Dahlberg, C. J., Decocq, G., Diekmann, M., Dynesius, M., Ejrnæs, R., Grytnes, J.-A., Hylander, K., Klanderud, K., ... Svenning, J.-C. (2013). Local temperatures inferred from plant communities suggest strong spatial buffering of climate warming across Northern Europe. *Global Change Biology*, 19(5), 1470-1481. <https://doi.org/10.1111/gcb.12129>
- Lenoir, J., Hattab, T., & Pierre, G. (2017). Climatic microrefugia under anthropogenic climate change: Implications for species redistribution. *Ecography*, 40(2), 253-266. <https://doi.org/10.1111/ecog.02788>
- Ma, Q., Su, Y., & Guo, Q. (2017). Comparison of Canopy Cover Estimations From Airborne LiDAR, Aerial Imagery, and Satellite Imagery. *IEEE Journal of Selected Topics in Applied Earth Observations and Remote Sensing*, 10(9), 4225-4236. <https://doi.org/10.1109/JSTARS.2017.2711482>
- Macek, M., Kopecký, M., & Wild, J. (2019). Maximum air temperature controlled by landscape topography affects plant species composition in temperate forests. *Landscape Ecology*, 34(11), 2541-2556. <https://doi.org/10.1007/s10980-019-00903-x>
- Maclean, I. M. D. (2020). Predicting future climate at high spatial and temporal resolution. *Global Change Biology*, 26(2), 1003-1011. <https://doi.org/10.1111/gcb.14876>
- Man, M., Kalčík, V., Macek, M., Brůna, J., Hederová, L., Wild, J., & Kopecký, M. (2023). myClim: Microclimate data handling and standardised analyses in R. *Methods in Ecology and Evolution*, 14(9). <https://doi.org/10.1111/2041-210X.14192>
- McCune, B., & Keon, D. (2002). Equations for potential annual direct incident radiation and heat load. *Journal of Vegetation Science*, 13(4), 603-606. <https://doi.org/10.1111/j.1654-1103.2002.tb02087.x>
- McLaughlin, B. C., Ackerly, D. D., Klos, P. Z., Natali, J., Dawson, T. E., & Thompson, S. E. (2017). Hydrologic refugia, plants, and climate change. *Global Change Biology*, 23(8), 2941-2961. <https://doi.org/10.1111/gcb.13629>
- Météo France. (2024). *Meteo.data.gouv.fr*. <https://meteo.data.gouv.fr/datasets>
- Naimi, B., Hamm, N. a s, Groen, T. A., Skidmore, A. K., & Toxopeus, A. G. (2014). Where is positional uncertainty a problem for species distribution modelling. *Ecography*, 37, 191-203. <https://doi.org/10.1111/j.1600-0587.2013.00205.x>

- Pastore, M. A., Classen, A. T., D'Amato, A. W., Foster, J. R., & Adair, E. C. (2022). Cold-air pools as microrefugia for ecosystem functions in the face of climate change. *Ecology*, *103*(8), e3717. <https://doi.org/10.1002/ecy.3717>
- Pebesma, E. (2018). Simple Features for R: Standardized Support for Spatial Vector Data. *The R Journal*, *10*(1), 439-446. <https://doi.org/10.32614/RJ-2018-009>
- Pérez-Navarro, M. Á., Serra-Díaz, J. M., Svenning, J., Esteve-Selma, M. Á., Hernández-Bastida, J., & Lloret, F. (2021). Extreme drought reduces climatic disequilibrium in dryland plant communities. *Oikos*. <https://doi.org/10.1111/oik.07882>
- Piedallu, C., Dallery, D., Bresson, C., Legay, M., Gégout, J.-C., & Pierrat, R. (2023). Spatial vulnerability assessment of silver fir and Norway spruce dieback driven by climate warming. *Landscape Ecology*, *38*(2), 341-361. <https://doi.org/10.1007/s10980-022-01570-1>
- Piqué, A., Pluck, P., Schneider, J.-L., & Whitechurch, H. (1994). The Vosges Massif. In J. Chantraine, J. Rolet, D. S. Santallier, A. Piqué, & J. D. Keppie (Éds.), *Pre-Mesozoic Geology in France and Related Areas* (p. 416-425). Springer. https://doi.org/10.1007/978-3-642-84915-2_32
- R Core Team. (2019). *R: A Language and Environment for Statistical Computing*. R Foundation for Statistical Computing. <https://www.R-project.org/>
- Raduła, M. W., Szymura, T. H., & Szymura, M. (2018). Topographic wetness index explains soil moisture better than bioindication with Ellenberg's indicator values. *Ecological Indicators*, *85*, 172-179. <https://doi.org/10.1016/j.ecolind.2017.10.011>
- Rey, D., & Neuhäuser, M. (2011). Wilcoxon-Signed-Rank Test. In M. Lovric (Éd.), *International Encyclopedia of Statistical Science* (p. 1658-1659). Springer. https://doi.org/10.1007/978-3-642-04898-2_616
- Richard, B., Dupouey, J.-L., Corcket, E., Alard, D., Archaux, F., Aubert, M., Boulanger, V., Gillet, F., Langlois, E., Macé, S., Montpied, P., Beaufiles, T., Begeot, C., Behr, P., Boissier, J.-M., Camaret, S., Chevalier, R., Decocq, G., Dumas, Y., ... Lenoir, J. (2021). The climatic debt is growing in the understory of temperate forests : Stand characteristics matter. *Global Ecology and Biogeography*, *30*(7). <https://doi.org/10.1111/geb.13312>
- Rita, A., Bonanomi, G., Allevato, E., Borghetti, M., Cesarano, G., Mogavero, V., Rossi, S., Saulino, L., Zotti, M., & Saracino, A. (2021). Topography modulates near-ground microclimate in the Mediterranean *Fagus sylvatica* treeline. *Scientific Reports*, *11*(1), 8122. <https://doi.org/10.1038/s41598-021-87661-6>
- Rolland, C. (2003). Spatial and Seasonal Variations of Air Temperature Lapse Rates in Alpine Regions. *Journal of Climate*, *16*(7), 1032-1046. [https://doi.org/10.1175/1520-0442\(2003\)016<1032:SASVOA>2.0.CO;2](https://doi.org/10.1175/1520-0442(2003)016<1032:SASVOA>2.0.CO;2)
- Sala, O. E., Chapin, F. S., Armesto, J. J., Berlow, E., Bloomfield, J., Dirzo, R., Huber-Sanwald, E., Huenneke, L. F., Jackson, R. B., Kinzig, A., Leemans, R., Lodge, D. M., Mooney, H. A., Oesterheld, M., Poff, N. L., Sykes, M. T., Walker, B. H., Walker, M., & Wall, D. H. (2000). Global biodiversity scenarios for the year 2100. *Science (New York, N.Y.)*, *287*(5459), 1770-1774. <https://doi.org/10.1126/science.287.5459.1770>
- Sanczuk, P., De Lombaerde, E., Haesen, S., Van Meerbeek, K., Luoto, M., Van der Veken, B., Van Beek, E., Hermy, M., Verheyen, K., Vangansbeke, P., & De Frenne, P. (2022). Competition mediates understory species range shifts under climate change. *Journal of Ecology*, *110*(8), 1813-1825. <https://doi.org/10.1111/1365-2745.13907>
- Sannier, C., Gallego, J., Langanke, T., Donezar, U., & Pennec, A. (2023). Tree cover area estimation in europe based on the combination of in situ reference data and the copernicus high resolution layer on tree cover density. *The International Archives of the Photogrammetry, Remote Sensing and Spatial Information Sciences*, *XLVIII-M-1-2023*, 277-284. <https://doi.org/10.5194/isprs-archives-XLVIII-M-1-2023-277-2023>
- Schweiger, A. H., Irl, S. D. H., Steinbauer, M. J., Dengler, J., & Beierkuhnlein, C. (2016). Optimizing sampling approaches along ecological gradients. *Methods in Ecology and Evolution*, *7*(4), 463-471. <https://doi.org/10.1111/2041-210X.12495>

- Serra-Diaz, J. M., Scheller, R. M., Syphard, A. D., & Franklin, J. (2015). Disturbance and climate microrefugia mediate tree range shifts during climate change. *Landscape Ecology*, 30(6), 1039-1053. <https://doi.org/10.1007/s10980-015-0173-9>
- Smith, S. A., Brown, A. R., Vosper, S. B., Murkin, P. A., & Veal, A. T. (2010). Observations and Simulations of Cold Air Pooling in Valleys. *Boundary-Layer Meteorology*, 134(1), 85-108. <https://doi.org/10.1007/s10546-009-9436-9>
- Stein, A., Gerstner, K., & Kreft, H. (2014). Environmental heterogeneity as a universal driver of species richness across taxa, biomes and spatial scales. *Ecology Letters*, 17(7), 866-880. <https://doi.org/10.1111/ele.12277>
- Thomas, A. L., Dambrine, E., King, D., Party, J. P., & Probst, A. (1999). A spatial study of the relationships between streamwater acidity and geology, soils and relief (Vosges, northeastern France). *Journal of Hydrology*, 217(1), 35-45. [https://doi.org/10.1016/S0022-1694\(99\)00014-1](https://doi.org/10.1016/S0022-1694(99)00014-1)
- Thuiller, W., Lavorel, S., Araújo, M. B., Sykes, M. T., & Prentice, I. C. (2005). Climate change threats to plant diversity in Europe. *Proceedings of the National Academy of Sciences*, 102(23), 8245-8250. <https://doi.org/10.1073/pnas.0409902102>
- Tichý, L. (2016). Field test of canopy cover estimation by hemispherical photographs taken with a smartphone. *Journal of Vegetation Science*, 27(2), 427-435. <https://doi.org/10.1111/jvs.12350>
- Tinya, F., Kovács, B., Bidló, A., Dima, B., Király, I., Kutszegi, G., Lakatos, F., Mag, Z., Márialigeti, S., Nascimbene, J., Samu, F., Siller, I., Szél, G., & Ódor, P. (2021). Environmental drivers of forest biodiversity in temperate mixed forests - A multi-taxon approach. *Science of The Total Environment*, 795, 148720. <https://doi.org/10.1016/j.scitotenv.2021.148720>
- Vandewiele, M., Geres, L., Lotz, A., Mandl, L., Richter, T., Seibold, S., Seidl, R., & Senf, C. (2023). Mapping spatial microclimate patterns in mountain forests from LiDAR. *Agricultural and Forest Meteorology*, 341, 109662. <https://doi.org/10.1016/j.agrformet.2023.109662>
- Vangansbeke, P., Máliš, F., Hédl, R., Chudomelová, M., Vild, O., Wulf, M., Jahn, U., Welk, E., Rodríguez-Sánchez, F., & Frenne, P. D. (2021). ClimPlant: Realized climatic niches of vascular plants in European forest understoreys. *Global Ecology and Biogeography*, 30(6), 1183-1190. <https://doi.org/10.1111/geb.13303>
- Venables, W. N., & Ripley, B. D. (2002). *Modern Applied Statistics with S* (Fourth). Springer. <https://www.stats.ox.ac.uk/pub/MASS4/>
- Vosper, S. B., & Brown, A. R. (2008). Numerical Simulations of Sheltering in Valleys: The Formation of Nighttime Cold-Air Pools. *Boundary-Layer Meteorology*, 127(3), 429-448. <https://doi.org/10.1007/s10546-008-9272-3>
- Wei, L., Sanczuk, P., De Pauw, K., Caron, M. M., Selvi, F., Hedwall, P., Brunet, J., Cousins, S. A. O., Plue, J., Spicher, F., Gasperini, C., Iacopetti, G., Orczewska, A., Uria-Diez, J., Lenoir, J., Vangansbeke, P., & De Frenne, P. (2024). Using warming tolerances to predict understory plant responses to climate change. *Global Change Biology*, 30(1), e17064. <https://doi.org/10.1111/gcb.17064>
- Wickham, H. (2011). Ggplot2. *WIREs Computational Statistics*, 3(2), 180-185. <https://doi.org/10.1002/wics.147>
- Wiens, J. J. (2016). Climate-Related Local Extinctions Are Already Widespread among Plant and Animal Species. *PLOS Biology*, 14(12), e2001104. <https://doi.org/10.1371/journal.pbio.2001104>
- Wild, J., Kopecký, M., Macek, M., Šanda, M., Jankovec, J., & Haase, T. (2019). Climate at ecologically relevant scales: A new temperature and soil moisture logger for long-term microclimate measurement. *Agricultural and Forest Meteorology*. <https://doi.org/10.1016/j.agrformet.2018.12.018>
- Zellweger, F., Braunisch, V., Morsdorf, F., Baltensweiler, A., Abegg, M., Roth, T., Bugmann, H., & Bollmann, K. (2015). Disentangling the effects of climate, topography, soil and

- vegetation on stand-scale species richness in temperate forests. *Forest Ecology and Management*, 349, 36-44. <https://doi.org/10.1016/j.foreco.2015.04.008>
- Zellweger, F., Coomes, D., Lenoir, J., Depauw, L., Maes, S. L., Wulf, M., Kirby, K. J., Brunet, J., Kopecký, M., Máliš, F., Schmidt, W., Heinrichs, S., den Ouden, J., Jaroszewicz, B., Buyse, G., Spicher, F., Verheyen, K., & De Frenne, P. (2019). Seasonal drivers of understorey temperature buffering in temperate deciduous forests across Europe. *Global Ecology and Biogeography*, 28(12), 1774-1786. <https://doi.org/10.1111/geb.12991>
- Zellweger, F., De Frenne, P., Lenoir, J., Rocchini, D., & Coomes, D. (2019). Advances in Microclimate Ecology Arising from Remote Sensing. *Trends in Ecology & Evolution*, 34(4), 327-341. <https://doi.org/10.1016/j.tree.2018.12.012>
- Zellweger, F., De Frenne, P., Lenoir, J., Vangansbeke, P., Verheyen, K., Bernhardt-Römermann, M., Baeten, L., Hédli, R., Berki, I., Brunet, J., Van Calster, H., Chudomelová, M., Decocq, G., Dirnböck, T., Durak, T., Heinken, T., Jaroszewicz, B., Kopecký, M., Máliš, F., ... Coomes, D. (2020). Forest microclimate dynamics drive plant responses to warming. *Science*, 368(6492), 772-775. <https://doi.org/10.1126/science.aba6880>
- Zuur, A. F., & Ieno, E. N. (2016). A protocol for conducting and presenting results of regression-type analyses. *Methods in Ecology and Evolution*, 7(6), 636-645. <https://doi.org/10.1111/2041-210X.12577>

8. Supplementary materials

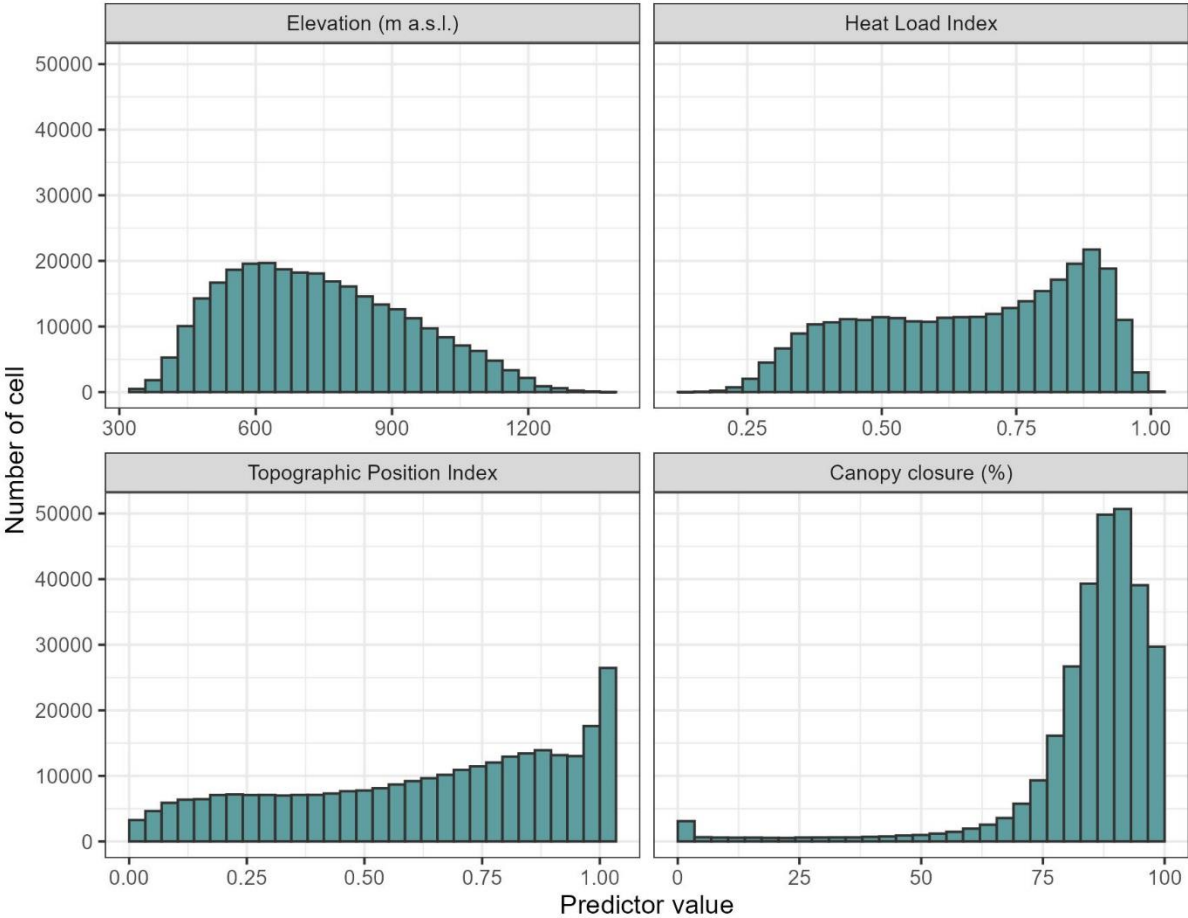


Figure S1: Distribution of the value of the four tested predictor of understory temperature thorough all the cells of the study region (forested cells of the Thur valley).

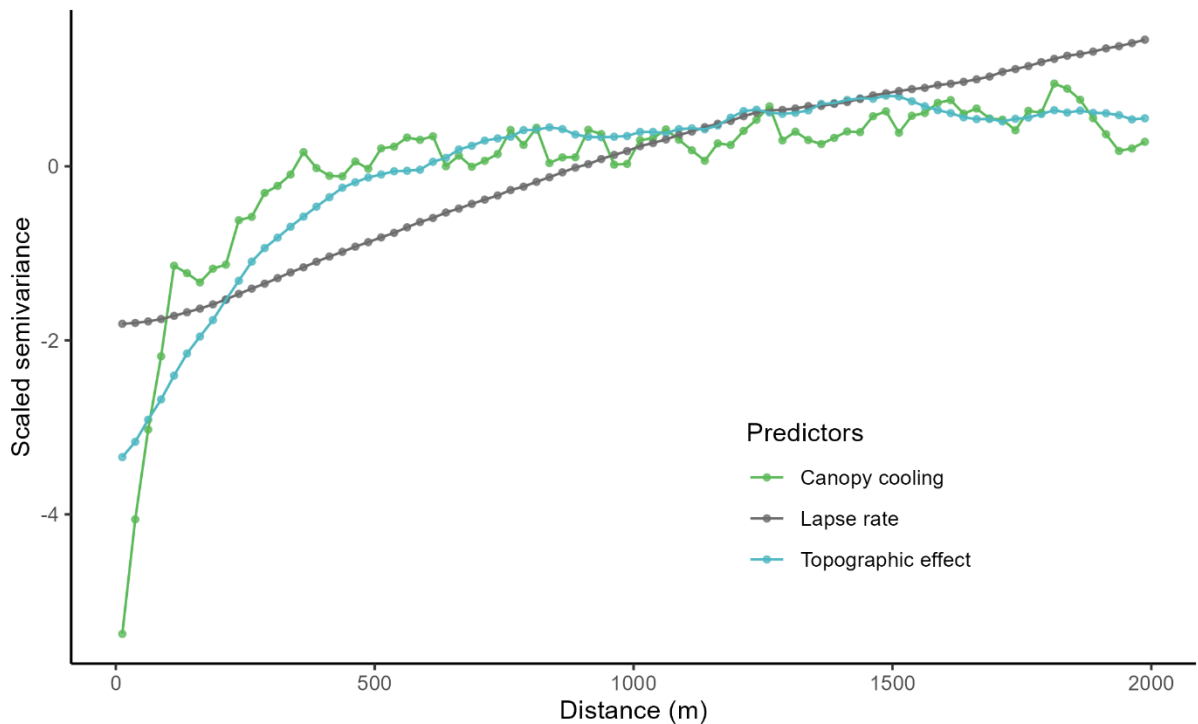


Figure S2: Variogram of the 3 maps of flora predictors (Figure 2), with a lag of 25m. Canopy cooling scale semivariance saturates first, followed by topographic effect and the lapse rate. The saturation of the lapse rate is not shown but is estimated at 6000 m.

Table S1: Summary of the sampling scheme. The left number represents the theoretical number of plots for the combination of targeted topographic feature and canopy closure (there were in total 8 strata), the right number represents the number of plots that had usable temperature data (logger found functioning). All other topographic feature aside from the targeted one were set to an intermediate value (nor high or low), read M&M 2.3 for more information on the sampling scheme.

		Canopy closure	
		Low (< 80%)	High (> 80%)
Heat Load Index	Low (< 0.6)	8 - 5	8 - 8
	High (> 0.7)	8 - 5	8 - 8
Topographic Position Index	Low (< 0.2)		8 - 7
	High (> 0.8)		8 - 6
Slope	Low (< 10°)		8 - 4
	High (> 25°)		8 - 5

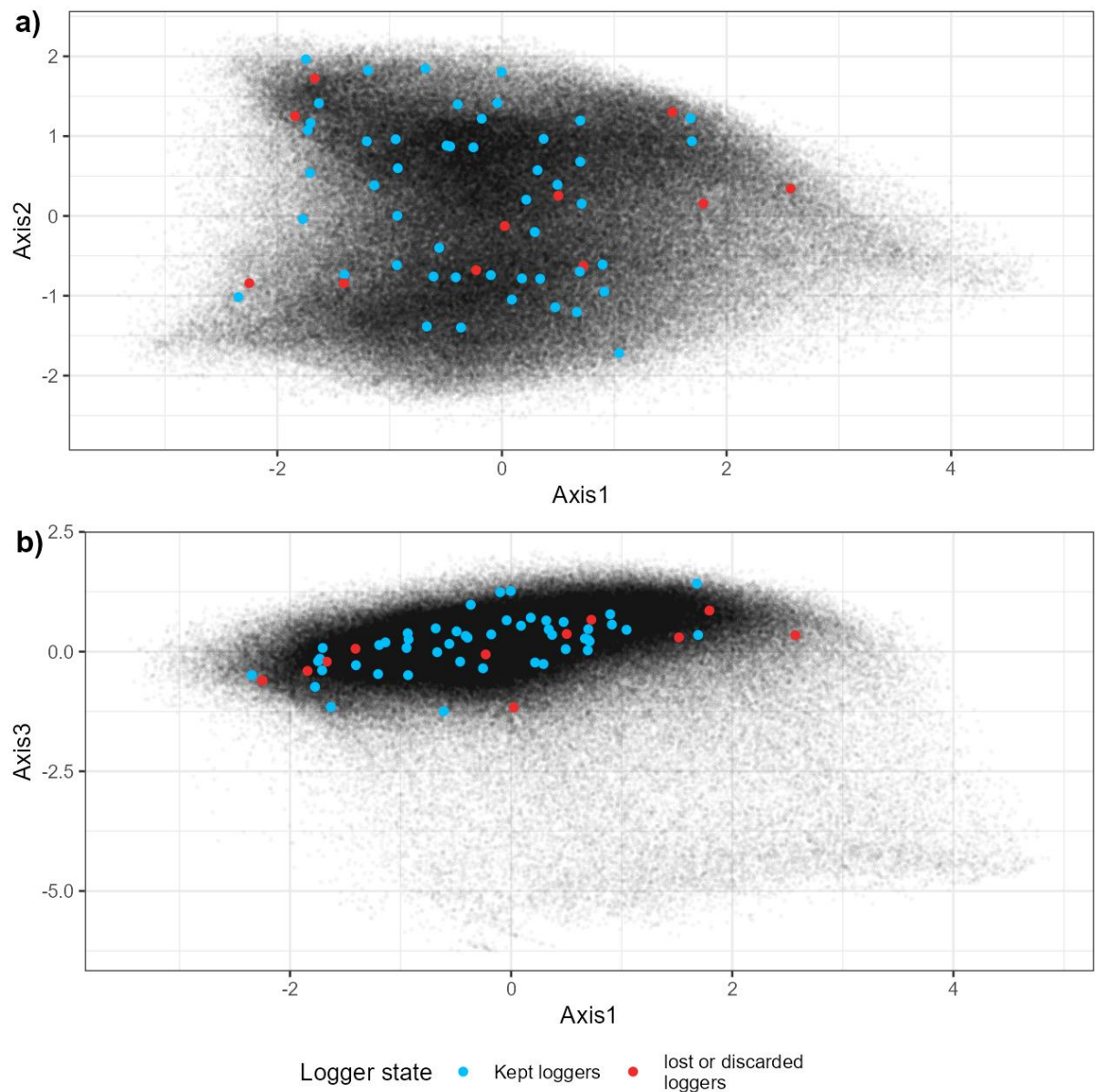


Figure S3; Principal component analysis of the spatial factor (Elevation, HLI, TPI, slope, canopy closure) ought to influence microclimate. Each point represents a forested cell (25m per 25 m, 289,733 cells) of the Thur Valley. Axis 1 is explained by elevation and topographic position (low values mean high elevation and TPI), Axis 2 represents mostly head load index (low values mean high HLI), Axis 3 represents mostly canopy cove (low values mean low canopy closure). The position in the PCA projection of the initial sampling and the final selection of loggers is shown (Lembrechts et al., 2021).

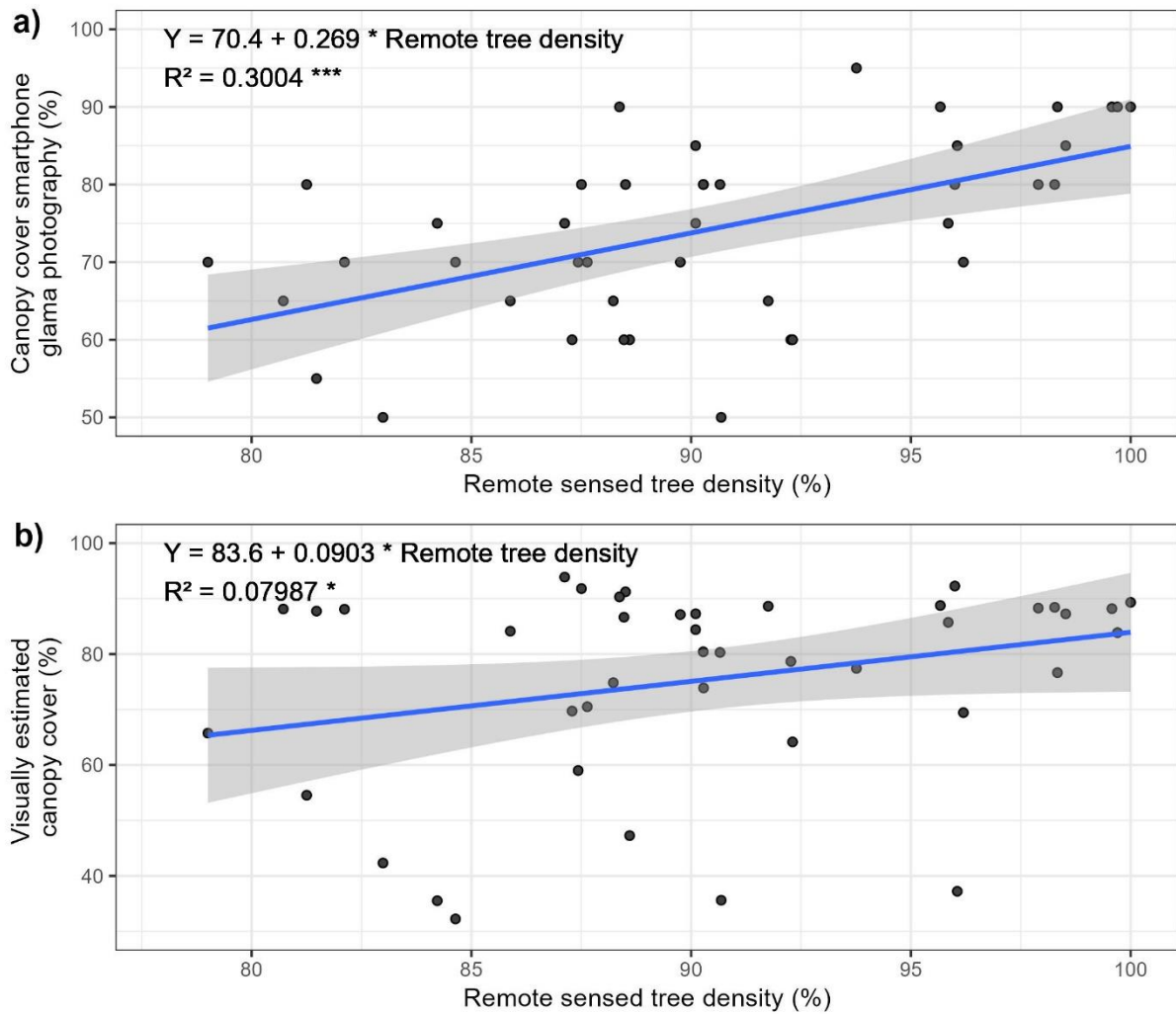


Figure S4: Relationship between Copernicus remote sensed tree density and canopy closure estimated in a 25-meter radius circle (a) and canopy cover estimated by a smartphone photography and segmented by the ‘Glama’ application (b). The blue line corresponds to a fitted linear model which equation, Person R^2 , and its statistical significance are displayed (***): $P < 0.001$, (*) $P < 0.1$. The ribbons are the confidence interval of the model.

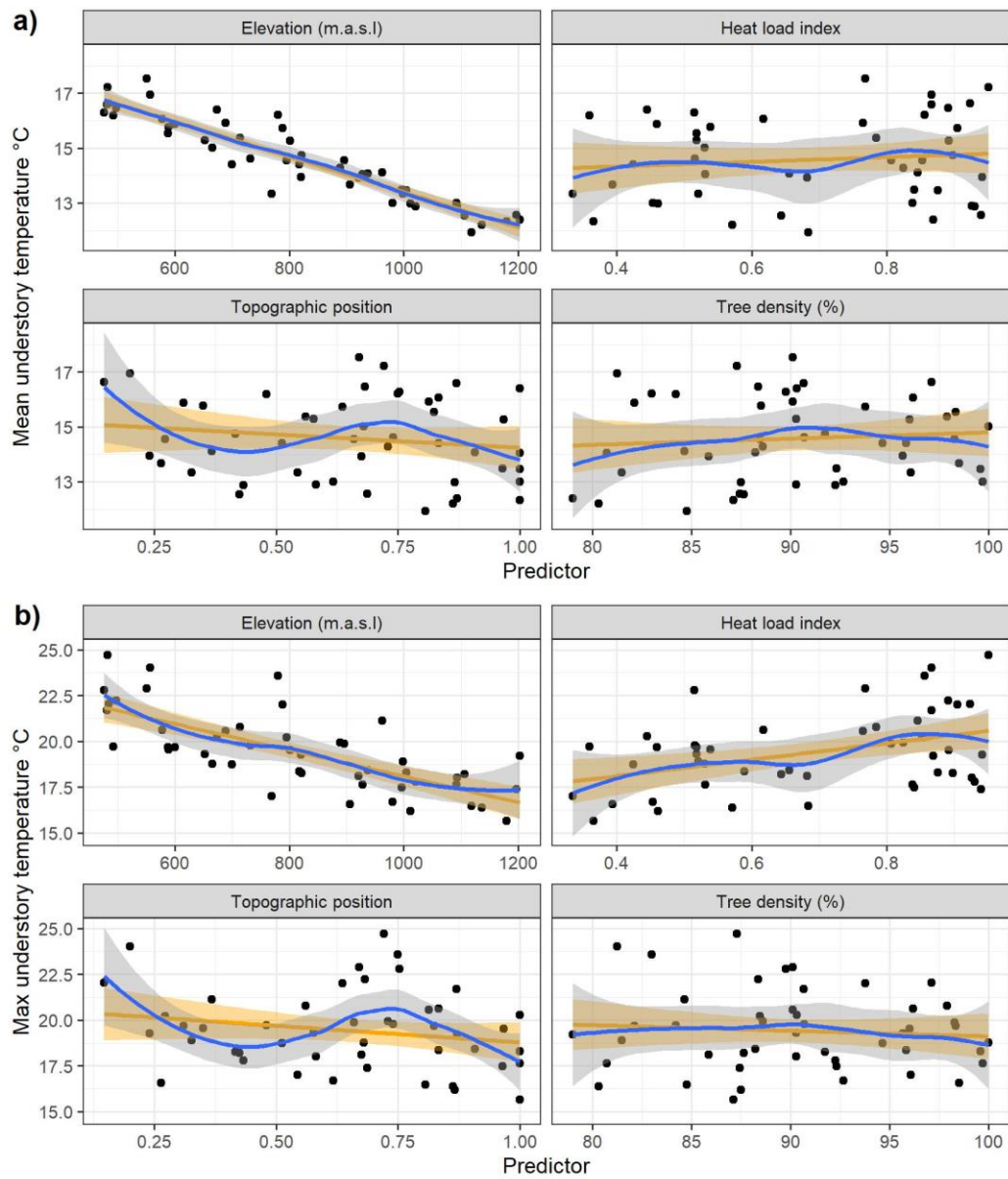


Figure S5: Relationship between mean (a) and maximum (b) understory temperature of the growing season with the 4 predictors of the linear temperature model. A loess smoother (blue) and an univariate linear model (orange) and their confidence interval are also displayed.

Table S2: Estimated parameters, their standard error and p-values of the predictors included in models of the field canopy closure daily mean growing season temperature. The range of the predictors in the calibration dataset and their standardized effect size on the temperature (standard deviation * estimate) are displayed. The percentage of explained variation per type of predictor is included. P-values were obtained with a Wald test on parameters.

Predictor	Type of predictor	Estimate	Standard error	Range	Effect size (°C)	Explained variation (%)	P-value
Intercept (°C)		19.2	0.605				<10 ⁻⁴
Elevation (m a.s.l.)	Elevation	-0.00656	0.000333	475 : 1203	-1.49	56.5	<10 ⁻⁴
Heat load index (n.u)	Topography	1.52	0.359	0.335 : 0.951	0.29	21.5	<10 ⁻⁴
Topographic index (n.u)		0.42	0.295	0.201 : 1	0.15		0.163
Canopy closure 25 radius (%)	Canopy	-0.00767	0.00599	50 : 95	-0.092	3.17	0.208

Table S3: Estimated parameters, their standard error and p-values of the predictors included in models of the immediate canopy closure (i.e. 'Glama' application) daily mean growing season temperature. The range of the predictors in the calibration dataset and their standardized effect size on the temperature (standard deviation * estimate) are displayed. The percentage of explained variation per type of predictor is included. P-values were obtained with a Wald test on parameters. The canopy cover was estimated visually in a 25-meter radius circle around the loggers. Immediate canopy cover was measured used a hemispherical photography above the logger and a sky segmentation application.

Predictor	Type of predictor	Estimate	Standard error	Range	Effect size (°C)	P-value
Intercept (°C)		16.2	0.812			<10 ⁻⁴
Elevation (m a.s.l.)	Elevation	-0.00672	0.000299	475 : 1203	-1.52	<10 ⁻⁴
Heat load index (n.u)	Topography	5.47	1.22	0.335 : 0.951		<10 ⁻⁴
Topographic index (n.u)	Topography	0.481	0.256	0.147 : 1	0.15	0.0682
Immediate canopy closure (%)	Canopy	0.0346	0.0109	32.23 : 93.88		0.00311
Topography index X Immediate canopy closure	Interaction	-0.0547	0.0162			0.00171

Table S4: Estimated parameters, their standard error and p-values of the predictors included in models of the daily maximum growing season temperature. The range of the predictors in the calibration dataset and their standardized effect size on the temperature (standard deviation * estimate) are displayed. The percentage of explained variation per type of predictor is included. P-values were obtained with a Wald test on parameters. Heat load and topographic indices have no units, refer to the methods for their calculation.

Predictor	Type of predictor	Estimate	Standard error	Range	Effect size (°C)	Explained variation (%)	P-value
Intercept (°C)		30.6	2.45				<10 ⁻⁴
Elevation (m a.s.l.)	Elevation	-0.00803	0.000685	475.69 : 1203.17	-1.77	56.5	<10 ⁻⁴
Heat load index (n.u)	Topography	5.35	0.732	0.335 : 0.951	1.05	21.5	<10 ⁻⁴
Topographic index (n.u)		0.333	0.607	0.147 : 1	0.081		0.587
Canopy closure (%)	Canopy	-0.0947	0.0253	79.004 : 100	-0.54	3.17	<10 ⁻⁴

Table S5: Estimated parameters, their standard error and p-values of the max temperature predictors of the community thermal index (CTI) linear model, and the species richness negative binomial generalized linear model. The range of the predictors and their standardized effect size on the community predicted variable (standard deviation * estimate) are displayed. The P-value is obtained by a Wald test on the parameter. (R² of the CTI model: 34.0%)

Model	Predictor	Estimate	Standard error	Range	Effect size	P-value
Species richness	Intercept (°C)	0.307	0.478	NA	NA	0.522
	Lapse rate (°C)	0.0351	0.0156	20.6 : 27.5	1.15	0.024
	Topography effect (°C)	-0.112	0.0271	1.79 : 5.36	-1.76	<10 ⁻⁴
	Canopy cooling (°C)	0.00365	0.035	-9.47 : -4.58	0.0464	0.917
	Bioindicator pH	0.413	0.032	3 : 7.15	7.97	<10 ⁻⁴
Community Thermal Index (°C)	Intercept (°C)	4.57	0.484	NA	NA	<10 ⁻⁴
	Lapse rate (°C)	0.0589	0.0156	20.6 : 27.5	0.106	<10 ⁻⁴
	Topography effect (°C)	0.0965	0.0273	1.79 : 5.36	0.0912	<10 ⁻⁴
	Canopy cooling (°C)	-0.00128	0.0356	-9.47 : -4.58	-0.00093	0.971
	Bioindicator pH	0.268	0.0313	3 : 7.15	0.243	<10 ⁻⁴

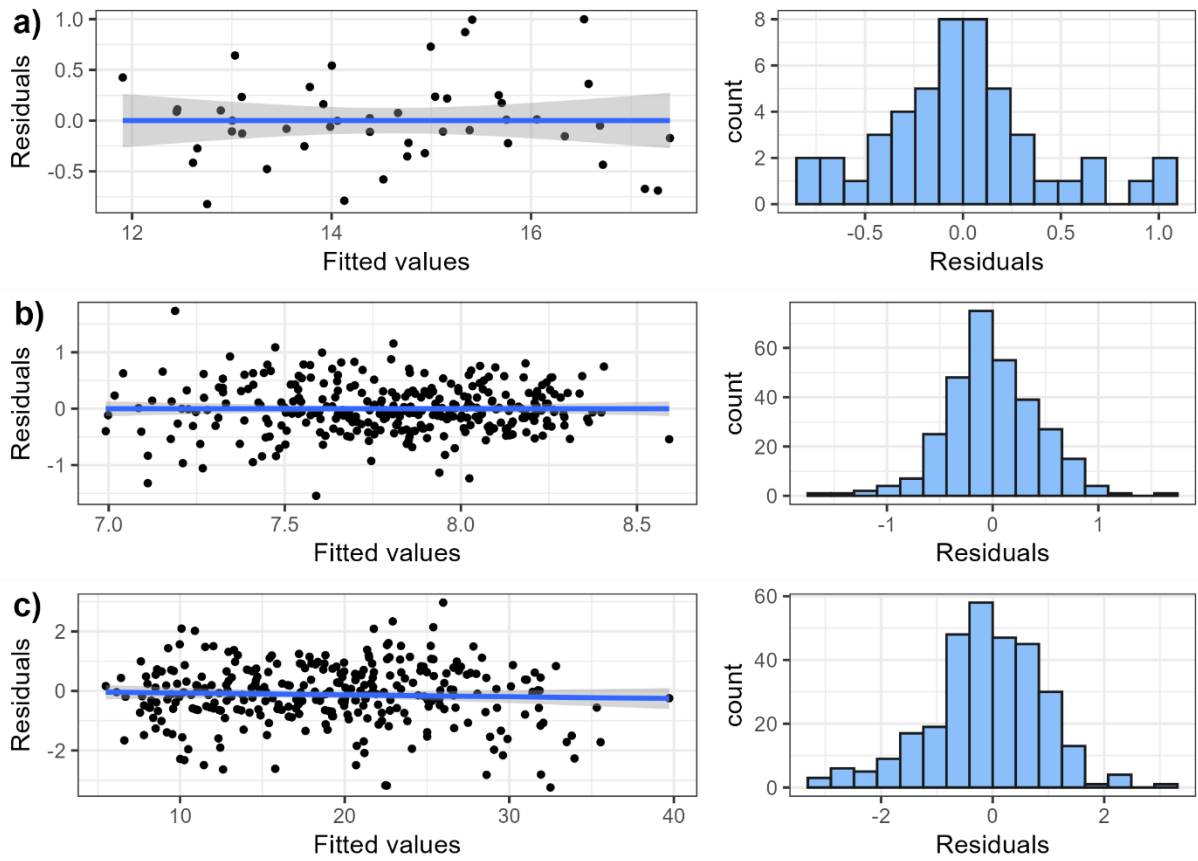


Figure S6: Relationship between residuals and fitted values, and histogram of residuals of the linear mean temperature model (a), the CTI linear model (b) and the species richness negative model (c).

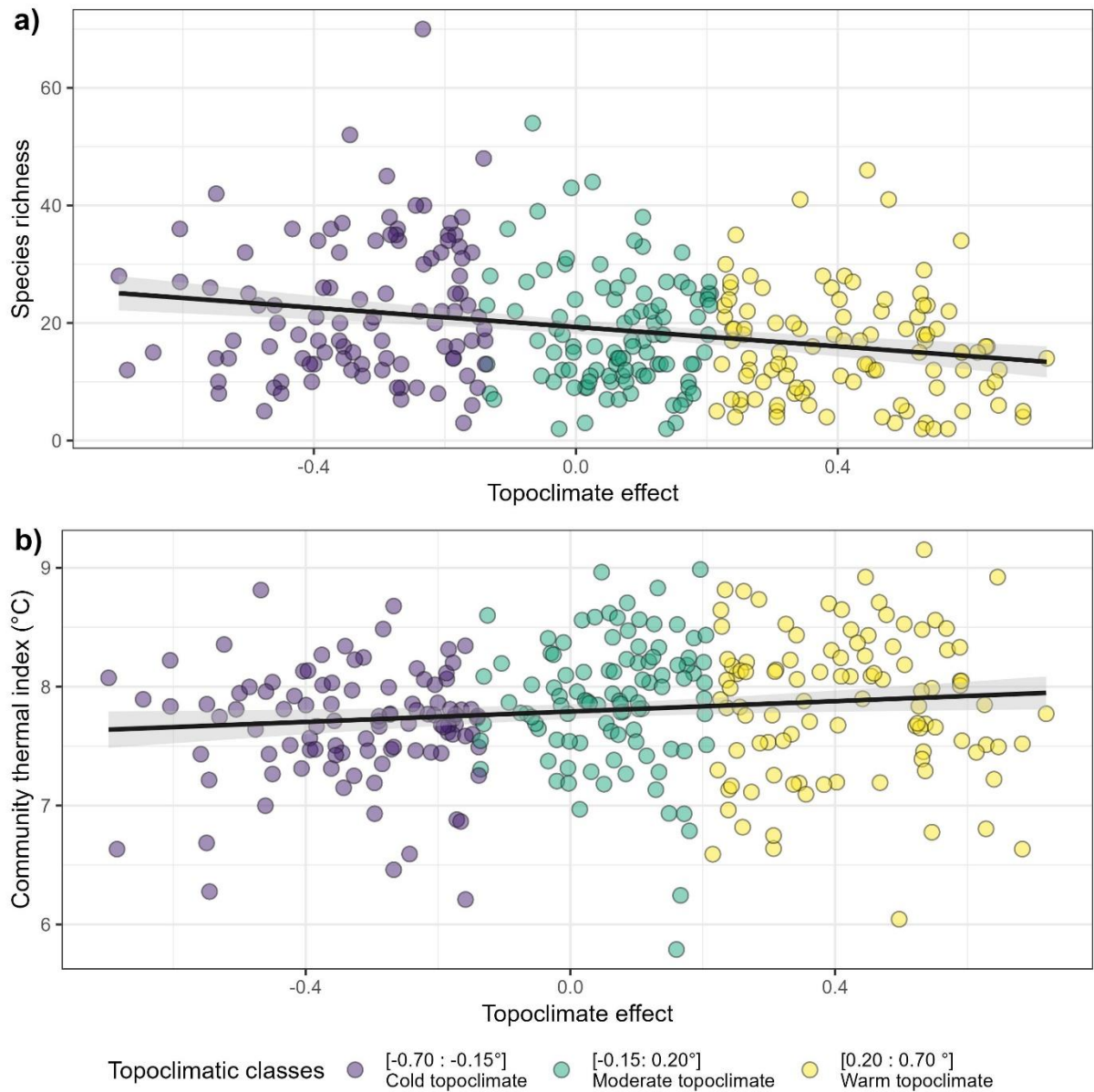


Figure S7 Species richness (a) and community thermal index (b) of 306 floristic surveys evenly spread into three topoclimatic buffering classes, as function of predicted topoclimatic effect on temperature (°C, compared to a moderate topographic situation).

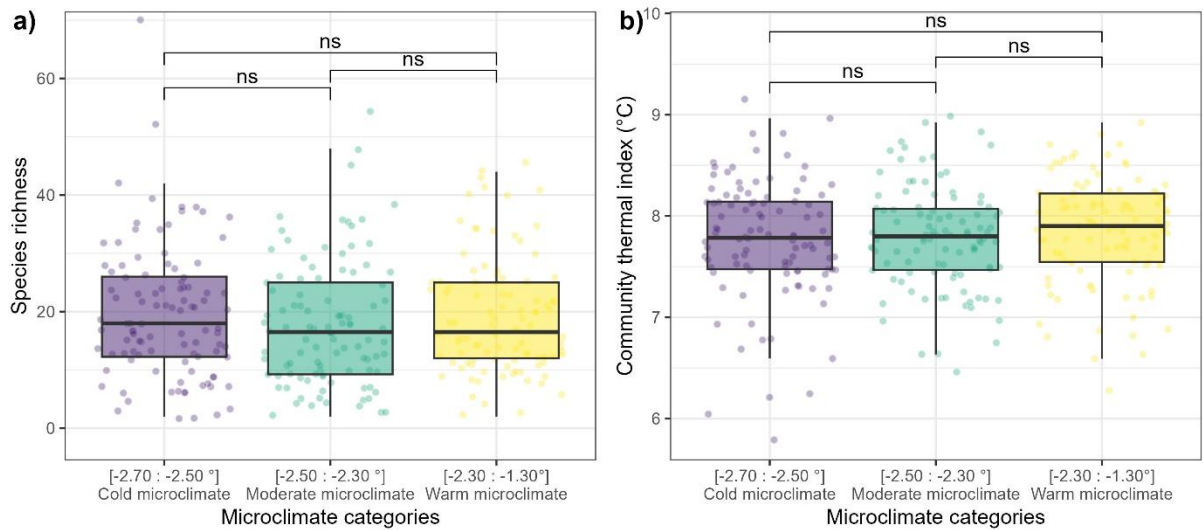


Figure S8: Species richness (a) and community thermal index (b) of 306 floristic surveys evenly spread into three microclimatic cooling classes. The p-value significance of a Wilcoxon test between two classes is displayed as follows: (ns): $p > 0.05$.

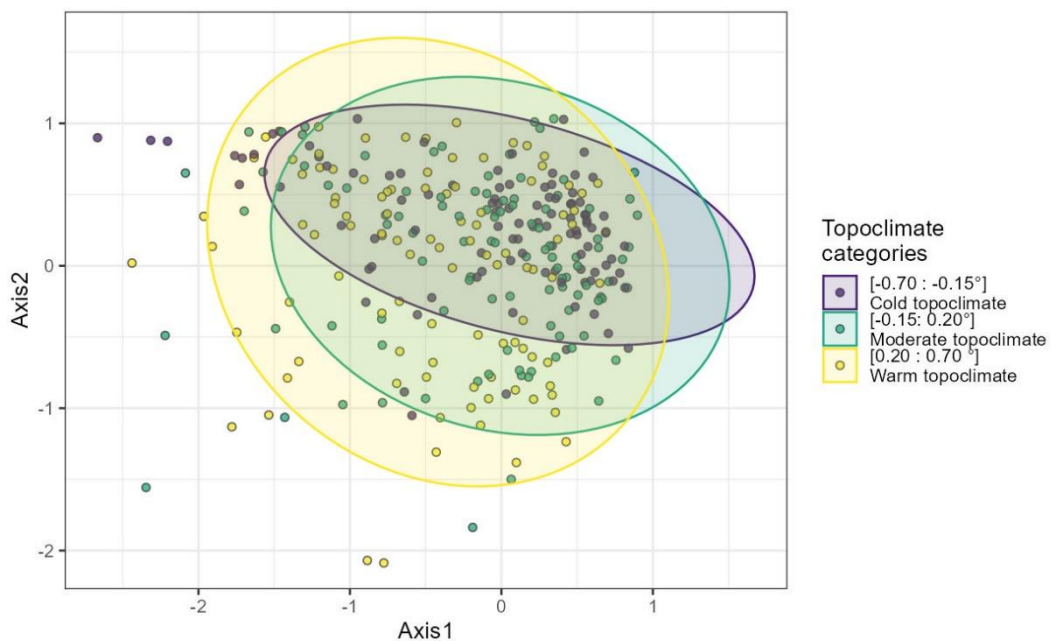


Figure S9: The first two axes of a correspondence analysis of the 306 floristic surveys spread among the three topoclimate cooling class.